SINGLE PASS COLLIDER MEMO CN-370

AUTHOR: Philip Bambade, Andrew Hutton DATE: February 1, 1989

TITLE: SPECIFICATION OF HARMONIC CORRE TIONS (*WIREFIX*) FOR THE SLC ARCS**

SLAC-CN--370

DE8J 007734

I. INTRODUCTION

In the original SLC commissioning plans, it was thought that accumulated optical mismatch, generated by focusing errors in the whole machine, would be corrected at the very end, in the Final Focus. Dedicated correctors for optical matching and a special adjustment strategy were planned for this purpose, with a large tuning range of up to about a factor four in any dimension of the beam phase-space[1].

For several reasons, this does not appear to be feasible. One major constraint limiting the magnitude of mismatches which can be absorbed in the Final Focus is the background generated in the detector, from electromagnetic debris and from muons produced when beam-tails strike apertures there. The apertures in the Final Focus, normalized to the nominal beam size, are in effect significantly smaller* than in the Arcs, both upstream and downstream of the dedicated optical correctors. Because of this, otherwise correctable optical distortions can result in enhanced backgrounds, as imperfectly collimated beam tails get magnified by the optical distortions, and can get scraped off.

With the present collimation and shielding arrangements, it is necessary to control the beam upstream of the Final Focus in order to inject a nearly matched phase-space there. Following work by Stiening in the Linac[2], and by Fieguth in the Arcs[3], we have developed and installed a new system of harmonic focusing corrections at the end of the SLC Arcs, to provide such control.

* The protection collimator PC18, for example, has a radius of 4 millimeters. After normalising by the nominal beam size, it is smaller than the Arc 6 millimeter vacuum chamber by a factor 6.7.

** Work supported by the Department of Energy Contract DE-AC03-76SF00515.

The scheme consists of introducing small regular and skew focusing deviations at specific harmonics of the betatron frequency which the phase-space is specially sensitive to. The harmonics in question are the zeroeth harmonic and the second harmonic of the betatron frequency*. The focusing deviations are introduced in the Arc lattice by perturbing the strengths of the combined function magnets with a set of appropriately rewired trim windings at their backleg†. The corrections provide an efficient way for adjusting both for errors in the Arc lattice and for mismatch at the injection to the Arc, generated by the upstream systems.

In this note, we describe the specification of this correction procedure as well as the present installation. Initial operational experience with this new method for adjusting beam-lines is presented elsewhere[4].

We begin with a description of the theoretical work which guided the specification. We then define the harmonics in the case of the Arc lattice, and describe the wiring modification and the strength of the regular and skew quadrupole components which can be generated, as calculated with POISSON[5]. We also describe the intra-magnet wiring arrangement through which the spatial strength modulations are produced.

Finally we present the predicted effects from the present installation, and outline possible improvements.

* In a circular accelerator, these harmonics correspond to the half-integer resonance in each plane, and to the sum and difference coupling resonances.

† The backleg windings were introduced in the Arc magnets originally to provide a step-wise adaptation of the strength of the lattice to the energy of the beam, which loses about 1 Gev through the emission of synchrotron radiation in the guide-field.

II. THEORY OF HARMONIC CORRECTIONS

II.1 Concept of Harmonic Correction in a Beam-Line[2,3]

In a beam-line where the focusing lattice consists of a periodic FODO array, the optical mismatch which occurs from focusing errors is conveniently described by an ellipse which rotates in phase-space with the betatron phase-advance[6]. Because ellipses are invariant under rotation of π, the beats in the beam envelope occur at twice the betatron frequency. Therefore, focusing errors which are separated by π, and more generally, which occur at twice the betatron frequency, will build up and enhance the optical mismatch.

Thus it is natural to consider adjusting the lattice and the phase-space in a FODO array by introducing controllable focusing perturbations at twice the betatron frequency. In general, the focusing errors in the lattice are random. Such focusing perturbations will thus add to or subtract from the strength of the Fourier component of the random errors which is at twice the betatron frequency. Controlling the strength of this harmonic thus enables to either make an overall correction of the lattice, or to purposely distort the lattice to minimize optical mismatch in the injected beam. This notion can be applied both to regular focusing errors and to skew focusing errors.

Because the perturbations from the errors are random and contain in general a systematic component, the accumulating optical mismatch will not remain indefinitely in phase with the focusing perturbations which are introduced. The longer the array, the larger the phase-shift between the two will be, and the weaker the effects from the controls become, as the system becomes more narrow-band. Because of this, harmonic corrections cannot be performed over a region that is too long, without losing much of their efficiency.

A second reason why harmonic corrections can in general not be applied over a region that is too long arises if the momentum dependance of the focusing, referred to as the chromaticity of the lattice, is not or is imperfectly corrected. In this case, the finite momentum spread in the beam will cause the optical mismatch from the focusing deviations to filament into a larger effective phase-space. The efficiency of a harmonic correction can in this case be reduced. Because the SLC Arcs are designed to be achromatic, such effects arise only to the extent the chromaticity-correction, because of the errors, is imperfect. For the range of errors which we

consider*, this is a small effect which we will not consider here.

II.2 Scope of Theory

The scope of this theoretical description is not that of full generality or rigor. The goal is rather to show the basic features of betatron oscillations and of transverse phase-space, as they are imaged through a FODO array which has been perturbed by a periodical focusing deviation. We will calculate the effects for each perturbation separately, in an idealized system with no errors, and ignore mixing effects which arise when several perturbations are applied simultaneously. Such mixing effects can change the magnitude of the effects, but do not change the basic features of the solutions which we will derive.

The only case of mixing which we will treat is that of a systematic focusing deviation, from the random errors or applied as an independent perturbation, combined with a periodic focusing perturbation at twice the betatron frequency. Rather than calculating the explicit solution for this case, we will indicate the magnitude of the reduction factor which results.

A practical case of periodic focusing deviation applied to a lattice with random errors will be explored through simulation in section VI.

In order to calculate the effects to be expected from harmonic focusing perturbations in a repetitive lattice, it is convenient to introduce and work with normalized variables.

II.3 Normalized Variables[7]

The transverse motion of a particle in a focusing array is governed by Hill's equation:

$$\ddot{z} + Kz = 0 \tag{1}$$

where $z = x, y$ and $s = ct$ are the transverse and longitudinal coordinates respectively, and where K represents the strength of the varying restoring force from the focusing array.

* We consider focusing perturbations of up to about one percent.

The use of the normalized variables $u_{x,y} = \frac{z}{\sqrt{\beta}}$ and $d\phi = \frac{ds}{\beta}$, where β satisfies:

$$\frac{1}{2}\beta\ddot{\beta} - \frac{1}{4}\dot{\beta}^2 + K\beta^2 - 1 = 0, \tag{2}$$

transforms (1) into the equation of a pure harmonic oscillator:

$$\ddot{u}_{x,y} + u_{x,y} = 0. \tag{3}$$

In (1) and (2), $\dot{f} \equiv \frac{df}{ds}$, where $f = z, \beta$. In (3), $\dot{u} \equiv \frac{du_{x,y}}{d\phi}$. The solution of (1) is thus:

$$z = a\sqrt{\beta}\cos(\phi + b), \tag{4}$$

where a and b are integration constants, and is referred to as a betatron oscillation. By definition the frequency of this oscillation, written as a function of the phase variable ϕ, is one.

Although the form in (4) is general, it is specially suited to periodic arrays consisting of repeated cells. In this case K, β and ϕ are periodic with the cell length and the betatron oscillation is pseudo-harmonic. An equivalent harmonic oscillator can be defined by sampling* (4) at each cell:

$$\begin{cases} z_n = a\sqrt{\beta}\cos(\phi_n + b), \\ \text{with} \quad \phi_n = n\mu. \end{cases} \tag{5}$$

where μ is the phase-shift per cell. In what follows, we consider perturbations of (3). The solutions we will derive coincide with those of (1) at the sampling points, after rescaling by $\sqrt{\beta}$. It is therefore possible to use (1) or (3) interchangeably, as long as one considers the restriction of the solution to the sampling points. We will use this fact to write simplified expressions for the perturbed motion.

II.4 Periodical Focusing Perturbations

II.4.1 Regular Quadrupole Perturbations

* From the sampling theorem, (4) is not undersampled by this procedure as long as the cell phase-shift is less than π, which is always the case[6]. In the SLC Arcs, $\mu = \frac{2\pi}{5}$.

To study the effect from a focusing modulation with regular quadrupoles, we replace K by $K + k\cos(\nu\phi + \psi)$ in the governing equation (1), where $k\cos(\nu\phi + \psi)$ represents a periodic deviation in the restoring force K, of amplitude k and of phase ψ, and with ν cycles per radians of phase-advance along the array. For the horizontal motion ($z = x$), the most important deviations are the ones in the focusing lenses. Conversely, for the vertical motion ($z = y$), the most important deviations are the ones in the defocusing lenses*. We consider small errors so that $k \ll K$.

In the normalized system, the equation of motion in (3) becomes:

$$\tilde{u}_{x,y} + (1 + g^r \cos(\nu\phi + \psi^r))u_{x,y} = 0, \tag{6}$$

with $g^r = \beta^2 k$, and $\psi^r = \psi$. The function β is sampled at the center of each focusing magnet for the horizontal motion, and at the center of each defocusing magnet for the vertical motion. Since only errors in the focusing (respectively defocusing) magnets affect the motion significantly in the horizontal (respectively vertical) planes, the factor g^r can be considered constants in (6).

II.4.2 Skew Quadrupole Perturbations

Similarly, we write the equations which govern the motion when focusing modulations with skew quadrupoles are applied. In this case, the restoring focusing force, proportional to the beam excursion in each transverse plane, acts on the perpendicular plane. This generates cross-plane coupling. The equations of motion are in this case:

$$\begin{cases} \tilde{u}_x + u_x + g^s \cos(\nu\phi + \psi^s)u_y = 0 \\ \tilde{u}_y + u_y + g^s \cos(\nu\phi + \psi^s)u_x = 0, \end{cases} \tag{7}$$

where g^s and ψ^s represent the amplitude and phase of the skew focusing modulation

* This results from the fact that in a FODO array, the beam size is naturally larger in each lens, in the plane in which the lens focuses. Because of this, the set of F and D magnets form close to orthogonal sets, in terms of their effect on the one-dimensional beam motion. A measure of this orthogonality is given by the ratio of the maximum to minimum beam size in the array. In the Arc lattice, this ratio is 2.8. The two sets are orthogonal for all practical purposes.

along the array†.

Defining $u_\pm = u_x \pm u_y$, we can rewrite (7) in a form similar to (6):

$$\ddot{u}_\pm + (1 \pm g^s \cos(\nu\phi + \psi^s))u_\pm = 0. \tag{8}$$

Next, we show that the perturbed motions, solutions of (6) and (7), are affected significantly only for two specific values of the frequency ν of the modulations, namely:

$$\nu \simeq 0 \quad \text{and} \quad \nu \simeq 2, \tag{9}$$

corresponding respectively to the systematic component in the errors and to the second harmonic of the betatron frequency.

II.5 First Order Solution

II.5.1 Method of Variation of Constants

Following Nayfeh, and along with the method of variation of constants, we

† The factor g^s can be related to the amplitude of skew quadrupole modulations in the focusing and in the defocusing magnets as follows:

$$g^s_{D,F} = \beta_{x,y}^{\frac{1}{2}} \beta_{y,x}^{\frac{1}{2}} k_{D,F},$$

where $k_{D,F}$ represent deviations to the focusing and defocusing magnet strengths in the regular coordinate system. The largest effect in the first (respectively second) of the two equations in (7) occurs in the defocusing (respectively focusing) magnet, since u_y (respectively u_x) is naturally the largest there. Therefore the term g^s in the first (respectively second) equation in (7) is essentially g^s_D (respectively g^s_F). Since in a FODO array, $\beta^F_{x,y} = \beta^D_{y,x}$, we have $g^s_D = g^s_F$. For this reason, we use the same g^s in the two equations in (7).

Furthermore, it has been shown (through computer simulation) that modulations where the skew quadrupole components have opposite signs in the focusing and in the defocusing lenses produce effects which cancel over one betatron period, except in the case of the systematic component, corresponding to $\nu \simeq 0$. For this reason, we use the same phase ψ^s in the two equations in (7). In the case $\nu \simeq 0$, skew quadrupole focusing perturbations with opposite sign in the focusing and in the defocusing magnets correspond to a rotation of the coordinate system. It can be shown that such a rotation can be expressed in the normalized variables by simply exchanging the sign of g^s in one of the two equations in (7)[9]. In this case, the two equations cannot be decoupled simply as in (8).

solve (6) and (7) by searching for solutions of the form[10]:

$$u = a\cos(\phi + \varphi)). \tag{10}$$

where a and φ are functions of ϕ to be determined. In (10) and in the rest of this paragraph, u represents $u_{x,y,+,-}$. By taking the first derivative of (10), letting a and ϕ vary, and by requiring that the result be what it would be if a and ϕ were constants (i.e. $\dot{u} = -a\sin(\phi + \varphi)$), an equation relating the first order derivatives $\dot{a}$ and $\dot{\varphi}$ is found. By calculating the second derivative of u, and after inserting it in an equation of the form of (6), we find a second equation relating $\dot{a}$ and $\dot{\varphi}$. Thus we have replaced a second order differential equation in u by two coupled first order differential equations in a and in φ. By solving this coupled system, we find that a and φ satisfy:

$$\begin{aligned}\frac{da}{a} &= \frac{g}{4}d\phi\sin[(2-\nu)\phi + 2\varphi - \psi] \\ &\quad + \sin[(2+\nu)\phi + 2\varphi + \psi], \qquad (11a)\\ d\varphi &= \frac{g}{4}d\phi(2\cos[\nu\phi + \psi] \\ &\quad + \cos[(2-\nu)\phi + 2\varphi - \psi] \\ &\quad + \cos[(2+\nu)\phi + 2\varphi + \psi]), \qquad (11b)\end{aligned}$$

where $\psi = \psi^{r,s}$ and $g = g^{r,s}$.

II.5.2 Averaging Method

To find the behavior of the solutions in the limit of small $g\phi$, we solve (11) to first order. To do so, we first note the fact that for values of $\nu \neq 0, 2$, the solutions of (11) are rapidly oscillating functions with amplitudes of order g. We will neglect such contributions, as they are bounded by g. Thus for $\nu \neq 0, 2$, the motion, solution of (6) and (7), is perturbed negligibly.

The amplitudes of the functions a and φ can only become significant if the functions on the right hand side of (11) are slowly varying functions. This occurs for $\nu \simeq 0, 2$.

From now on, we will write g_0 for the magnitude of the systematic focusing deviations, corresponding to $\nu \simeq 0$, and g_2 and ψ_2 for the amplitude and phase of focusing modulations at twice the betatron frequency, corresponding to $\nu \simeq 2$.

We first solve for $\nu \simeq 0$. The solution is obtained by integration of (11b). This gives:

$$u \simeq a_0 \cos[(1 + \frac{g_0}{2})\phi + \varphi_0], \tag{12}$$

where a_0 and φ_0 are integration constants.

Next we solve for $\nu \simeq 2$, integrating this time both (11a) and (11b). From (11b), and including only the slowly varying term $\cos[(2-\nu)\phi + 2\varphi - \psi_2]$, we note that $d\varphi \leq \frac{1}{4} g_2 d\phi$. The total variation of φ over the interval of integration is thus bounded by $\frac{1}{4} g_2 \phi$. Thus the right hand sides of (11) stay about constant if $\frac{1}{4} g_2 \phi \ll \pi$. We can in this case treat the slowly varying terms on the right hand side of (11) as constants in the integration. We obtain in this case:

$$u \simeq a_0 e^{\lambda \phi} \cos[(1+\kappa)\phi + \varphi_0]. \tag{13}$$

where:

$$\begin{cases} \lambda = \frac{g_2}{4} \sin(2\varphi_0 - \psi_2), \\ \kappa = \frac{g_2}{4} \cos(2\varphi_0 - \psi_2). \end{cases} \tag{14}$$

II.6 Physical Description of Perturbed Motion

II.6.1 One-Dimensional Oscillations

From (14), (15) and (16), we characterize the effect of regular focusing modulations on the one-dimensional motion, in the limit of small perturbation, as follows:

Case $\nu \simeq 0$:

The fundamental frequency of the oscillations is shifted by systematic regular focusing deviations, corresponding to $\nu = 0$. This shift is independent of the initial phase of the betatron oscillation.

Case $\nu \simeq 2$:

The amplitude and frequency of the oscillations are perturbed resonantly by regular focusing modulations at the second harmonic of the fundamental betatron frequency, corresponding to $\nu = 2$. Depending on the phase ψ_2 of this modulation and on the initial phase φ_0 of the betatron oscillation, the amplitude will initially decay or grow exponentially with a growth rate λ, and the frequency will increase

or decrease linearly by the slippage parameter κ. These two effects are out of phase: maximum frequency-slippage coincides with a constant amplitude, and zero frequency-slippage with a maximally perturbed amplitude*.

We will describe the consequences for the phase-space and for the beam envelope in the next section.

II.6.2 Two-Dimensional Oscillations

Case $\nu \simeq 0$: (Systematic Skew Component)

We can use (12) and $u_{\pm} = u_x \pm u_y$ to calculate the effects from systematic skew perturbation. We obtain:

$$u_x \simeq [u_x(0)\cos\phi + \dot{u}_x(0)\sin\phi]\cos g_0^s\phi + [-u_y(0)\sin\phi + \dot{u}_y(0)\cos\phi]\sin g_0^s\phi \qquad (15a)$$

and:

$$u_y \simeq [-u_x(0)\sin\phi + \dot{u}_x(0)\cos\phi]\sin g_0^s\phi + [u_y(0)\cos\phi + \dot{u}_y(0)\sin\phi]\cos g_0^s\phi \qquad (15b)$$

The results in (15a) and (15b) show that in the case of a systematic skew focusing perturbation ($\nu \simeq 0$), oscillations originating in one plane are gradually transferred into the other plane, and that the sum of squares of the oscillation amplitudes in both planes remains constant. Thus there is beating between the two planes. The period of this beating is determined by g. This is true for both the positions $u_{x,y}$ and the angles $\dot{u}_{x,y}$, as can be seen from differentiating (15). Therefore the beating phenomenon which arises is between the two full phase-spaces in both planes.

Case $\nu \simeq 0$: (Coordinate Rotation)

The solutions are in this case simple harmonic oscillators, in the rotated coordinate system. We will not write these solutions explicitly.

Case $\nu \simeq 2$:

* The separation between the two initial phases φ_0, corresponding to maximum growth or decay, and to maximum phase-slippage, depends on the magnitude of the perturbation. It is strictly 45 deg only in the limit of small perturbation. We will describe the behavior for larger perturbation in the next section.

From (8) and (13), the form of the solutions are:

$$u_{\pm} = a_0^{\pm} e^{\lambda_{\pm}\phi} \cos[(1 \pm \kappa_{\pm}\phi + \varphi_0^{\pm}]. \tag{16}$$

For initial conditions contained in one of two $u_x, \dot{u}_x$ or $u_y, \dot{u}_y$ planes, corresponding to the propagation of betatron oscillations launched from one plane at a time (for example: $u_y(0) = \dot{u}_y(0) = 0$), one can show that the solutions can be written as the sum of two functions, one exponentially growing and one exponentially decaying:

$$u_{x,y} = \frac{a_o}{2}[e^{\lambda\phi} \cos[(1+\kappa)\phi + \varphi_0] \pm e^{-\lambda\phi} \cos[(1-\kappa)\phi + \varphi_0]]. \tag{17}$$

In this case, the oscillations will grow exponentially in both planes for arbitrary initial phase.

It is however possible to find initial conditions such that both u_+ and u_- decay simultaneously initially. This has been shown independently by solving (8) numerically[9]. One example of such initial conditions is $u_x(0) = \dot{u}_x(0) = u_y(0) = \dot{u}_y(0)$.

In the next section, we will analyse the consequences from this cross-plane coupling on the areas of the beam phase-space, projected in each plane (projected emittances), and for the beam envelopes, in each of the above cases.

II.7 Physical Description of Perturbed Phase-Space

II.7.1 Matched Phase-Space

In the case of a perfect lattice and when the beam phase-space is matched at the input, it remains matched as it is imaged through the array by the optics.

The equation of the envelope of the matched phase-space is easily constructed from the form of the betatron oscillation in (4). One obtains an ellipse:

$$\gamma z^2 + 2\alpha z\dot{z} + \beta \dot{z}^2 = a^2, \tag{18a}$$

where $\dot{z} = \frac{dz}{ds}$, $\gamma = \frac{1+\dot{\beta}^2}{\beta}$, and $\alpha = \frac{-\dot{\beta}}{2}$. The quantity in (18a) is called the Courant-

Snyder invariant[7]. It can also be written in matrix form:

$$(z,\dot{z})\mathrm{T}^{-1}\begin{pmatrix} z \\ \dot{z} \end{pmatrix} = a^2, \text{where } \mathrm{T} = \begin{pmatrix} \beta & -\alpha \\ -\alpha & \gamma \end{pmatrix} \text{ and } \det(\mathrm{T}) = 1. \qquad (18b)$$

The equations in (18) also define the closed phase-space trajectory of a particle with initial condition a. The parameters α, β and γ are called Twiss parameters. They characterize the lattice. They also describe the beam phase-space if and when it is matched to the lattice. In this case, the beam-matrix[11] $\sigma = \epsilon\mathrm{T}$. The area πa^2 of the ellipse is identified as π times the emittance ϵ.

In the normalized coordinates $u = \frac{z}{\sqrt{\beta}}$ and $\dot{u} = \frac{\dot{z}\sqrt{\beta}}{\dot{\phi}} = \sqrt{\beta}(\dot{z} - \frac{\dot{\beta}}{2\beta}z)$ defined in II.3, the matched phase-space is a circle of radius ϵ. This can be verified by direct substitution in (18a).

II.7.2 Perturbed One-Dimensional Phase-Space

Case $\nu \simeq 0$:

In II.6.1, we described the effect of a systematic regular focusing deviation, with magnitude g_0^r, corresponding to $\nu \simeq 0$. The motion is in this case simply frequency-shifted, and the solutions in (12) will satisfy the equation of the matched circle defined in II.7.1. The beam phase-space remains in this case matched*.

Case $\nu \simeq 2$:

When the lattice is perturbed by focusing errors, this matched circle is distorted into an ellipse. We describe this condition of the beam phase-space by mismatch. We characterize this mismatch by the ratio M of the radius of the larger circle in which this ellipse is inscribed to that of the initial circle corresponding to the matched case, and by the angle ϕ_0 between its major axis and the abscissa (see Fig. 1): M and ϕ_0 are the amplitude and the phase of the mismatch.

---

* This is strictly speaking only approximately true, as the Twiss parameters in (18b), which characterize the FODO array, depend on the phase advance per cell. For example, it can be shown that for a thin lens FODO array[13]:

$$\beta_{\pm} = L\frac{1 \pm \sin(\mu/2)}{\sin\mu},$$

where $\beta_{\pm}$ are the maximum and minimum values, occurring in each plane in the lenses which are focusing, and respectively defocusing, in that plane. For small systematic perturbations of up to one percent, the variation of the Twiss parameters is of the order of one percent. We neglect such variations.

In II.6.1, we described the effect of a regular focusing modulation at twice the betatron frequency, with magnitude g_2^r and with phase ψ_2^r, corresponding to $\nu \simeq 2$. We found that the maximum oscillation amplitude which can be reached is: $u_{max} = e^{\frac{g_2^r}{4}\phi}$.

The phase ϕ_0 of the mismatch depends on how far along the array the mismatch has propagated, i.e. on the accumulated phase advance ϕ, and on the phase ψ_2^r of the regular focusing modulation. We can thus write:

$$\phi_0 = \phi + \psi_2^r. \tag{19}$$

Since ϕ_0 can take an arbitrary value, we can identify:

$$M = u_{max} = e^{\frac{g_2^r}{4}\phi}. \tag{20}$$

The equation of the distorted ellipse is calculated in terms of M and ϕ_0, first in the coordinates rotated by ϕ_0 in which it is erect, and then transforming back into the unrotated coordinates. This gives:

$$u^2(M^2\cos^2\phi_0 + \frac{1}{M^2}\sin^2\phi_0) + \dot{u}^2(M^2\sin^2\phi_0 + \frac{1}{M^2}\cos^2\phi_0) + 2u\dot{u}\cos\phi_0\sin\phi_0(M^2 - \frac{1}{M^2}) = \epsilon. \tag{21}$$

The corresponding beam-matrix, written in the normalized system, in terms of the amplitude g_2^r and of the phase ψ_2^r, is:

$$\Sigma_{g_2^r,\psi_2^r}(\phi) = \epsilon \begin{pmatrix} \Sigma_{11} & \Sigma_{12} \\ \Sigma_{12} & \Sigma_{22} \end{pmatrix}, \tag{22}$$

where:

$$\begin{cases} \Sigma_{11} = \cosh(\frac{g_2^r}{2}\phi) + \sinh(\frac{g_2^r}{2}\phi)\cos(2\phi + \psi_2^r) \\ \Sigma_{12} = -\sinh(\frac{g_2^r}{2}\phi)\sin(2\phi + \psi_2^r) \\ \Sigma_{22} = \cosh(\frac{g_2^r}{2}\phi) - \sinh(\frac{g_2^r}{2}\phi)\cos(2\phi + \psi_2^r), \end{cases} \tag{23}$$

and where ϵ is the emittance. Transforming back into real coordinates gives:

$$\begin{cases} \sigma_{11} = \beta\Sigma_{11}, \\ \sigma_{12} = \Sigma_{12} - \alpha\Sigma_{11}, \\ \sigma_{22} = \frac{1}{\beta}(\Sigma_{22} + \alpha^2\Sigma_{11} - 2\alpha\Sigma_{12}). \end{cases} \tag{24}$$

For the ideal lattice, characterized by $g_2^r = 0$, (24) reduces to (18b) as expected.

In summary, when the lattice is perturbed by a regular focusing modulation at twice the betatron frequency, with amplitude g_2^r and phase ψ_2^r, the phase-space gradually becomes elongated into an ellipse with a major axis which grows exponentially with the accumulated phase advance, at a growth rate $\frac{g_2^r}{2}$. This ellipse rotates in phase-space at the betatron frequency. The initial value of the phase of the mismatch is determined by the phase ψ_2^r.

From (23), we see that the beam size beats between minimum and maximum values, of $e^{-\frac{g_2^r}{2}\phi}$ and $e^{\frac{g_2^r}{2}\phi}$ respectively. The beating occurs with a period of π, as illustrated in Fig. 1. Equation (23) (and graphically Fig. 1) also allows us to study the behavior of the solutions, both for large and for small perturbation. For small perturbation ($g_2^r\phi \ll 1$), the first equation in (23) reduces to $\Sigma_{11} \simeq 1 + \frac{g_2^r\phi}{2}\cos(2\phi + \psi_2^r)$. In this case, the separation in the phase ϕ between maximally growing or decaying solutions, and solutions with an unperturbed amplitude (corresponding to $M = 1$), is exactly 45 deg. This is in agreement with the results from the first order calculations described in II.6.1. For larger $g_2^r\phi$, the initial phases corresponding to an unperturbed amplitude move closer and closer to the phase corresponding to a maximally decaying solution. For infinite g_2^r, all solutions become eventually exponentially growing, except for the "single" one for which, strictly, $\cos(2\phi+\psi_2^r) = -1$. This has been shown independently by solving (6) numerically[9].

II.7.3 Coupled Two-Dimensional Phase-Space

In II.6.2, we gave expressions describing the cross-coupling of betatron oscillations which occurs from systematic skew focusing errors, corresponding to $\nu \simeq 0$, and from skew focusing modulations at twice the betatron frequency, corresponding to $\nu \simeq 2$. We use these expressions to infer the evolution of the areas of the phase-space projections in each plane. The correctness of all forms (except (28)) given in this section has been verified through simulation. Results from these simulations are presented in section IV.

We assume an input phase-space where the horizontal and vertical planes are not coupled, but where the emittances are not necessarily equal. Let $r = \epsilon_y/\epsilon_x$

be the ratio of the initial vertical to the initial horizontal emittances (we assume $r \leq 1$), and let us normalize the results to the initial horizontal emittanc , by putting $\epsilon_x(\phi = 0) = 1$.

Case $\nu \simeq 0$: (Systematic Skew Component)

In this case, it is possible to calculate, from (15), the projected emittances, as the beam is imaged through the array. We obtain:

$$\begin{cases} \epsilon_x(\phi) = \frac{1}{2}[(1+r) + (1-r)\cos g_0^s \phi] \\ \epsilon_y(\phi) = \frac{1}{2}[(1+r) - (1-r)\cos g_0^s \phi]. \end{cases} \tag{25}$$

Putting $r = 0$ in (25) shows explicitly the beating phenor which we described in II.6.2. One obtains in this case:

$$\begin{cases} \epsilon_x(\phi) = \cos^2(g_0^s \phi) \\ \epsilon_y(\phi) = \sin^2(g_0^s \phi) \end{cases} \tag{26}$$

The sum of the two emittances is in this case constant, and transverse oscillation energy is transferred back and forth between one plane and the other. This condition describes adequately the imaging of betatron oscillations launched from one plane at a time.

In the special case of equal emittances, corresponding to $r = 1$, we have from (25) that:

$$\epsilon_x(\phi) = \epsilon_y(\phi) = 1. \tag{27}$$

The motion remains in this case unperturbed by systematic skew focusing deviations.

For an arbitrary value of r, the two emittances will beat between minimum and maximum values of r and 1. As can be seen, the variations of the two emittances are out of phase.

Case $\nu \simeq 0$: (Coordinate Rotation)

In this case, the projected emittances are calculated by transforming a four-dimensional uncoupled beam-matrix through a rotation of the coordinate system. We obtain:

$$\begin{cases} \epsilon_x(\phi) = \cos^2(2g_0^s) + r\sin^2(2g_0^s) \\ \epsilon_y(\phi) = \sin^2(2g_0^s) + r\cos^2(2g_0^s). \end{cases} \tag{28}$$

The same features apply as for the systematic skew component: for $r = 0$, the

sum of the projected emittances is preserved, and for $r = 1$, the phase-space is not perturbed.

Case $\nu \simeq 2$:

In this case, we write, by analogy with (25):

$$\begin{cases} \epsilon_x(\phi) = \cosh^2 \frac{g_2'}{4}\phi + r^2 \sinh^2 \frac{g_2'}{4}\phi \\ \epsilon_y(\phi) = \sinh^2 \frac{g_2'}{4}\phi + r^2 \cosh^2 \frac{g_2'}{4}\phi. \end{cases} \tag{29}$$

In the special case of zero initial emittance in the vertical plane ($r = 0$), we obtain:

$$\begin{cases} \epsilon_x(\phi) = \cosh^2(\frac{g_2}{4}\phi) \\ \epsilon_y(\phi) = \sinh^2(\frac{g_2}{4}\phi), \end{cases} \tag{30}$$

in accordance with (17), from which all solutions grow exponentially if the initial conditions are restricted to one plane.

The difference between the two emittance projections is in this case constant, and the projected emittances grow exponentially in both planes. This condition describes adequately the imaging of betatron oscillations launched from one plane at a time

In the special case of equal initial emittances in each plane (r=1), we obtain:

$$\epsilon_x(\phi) = \epsilon_y(\phi) = \cosh \frac{g_2'}{2}\phi. \tag{31}$$

The two projected emittances remain in this case equal, and grow exponentially*.

II.8 Summary Description - Number of Independent Perturbations

Thus we find that, in total, the transverse motion can be perturbed by ten independent parameters:

* Although the envelope grows, there can exist, as we found in (16), individual solutions which are decaying.

1. The one-dimensional horizontal motion can be perturbed in three ways, namely through a systematic strength deviation in the focusing quadrupoles, and through the amplitude and phase of a periodic focusing deviation at twice the betatron frequency in the focusing quadrupoles.

2. The one-dimensional vertical motion can be perturbed in three ways, namely through a systematic strength deviation in the defocusing quadrupoles, and through the amplitude and phase of a periodic focusing deviation at twice the betatron frequency in the defocusing quadrupoles.

3. The two-dimensional coupled motion can be perturbed in four ways, namely through a systematic skew quadrupole component, through the amplitude and phase of a periodic skew focusing deviation at twice the betatron frequency†, and through an overall coordinate rotation.

These ten perturbations correspond to the number of free parameters in a fully general two-dimensional transfer matrix[13].

To the extent that the errors are small and that only one perturbation is applied at a time, it is possible to simply parametrize the perturbed motion as a function of these ten parameters, as was shown above. In general, however, a full parametrization will be complicated as the mixing between the perturbations, not considered here, will yield higher order dependances.

In the case of the four-dimensional beam phase-space, it would appear from our calculations that it only can be perturbed in seven independent ways, since the two systematic strength deviations, in the focusing and in the defocusing magnets, do not distort the phase-space, and since the coupling effect from the overall coordinate rotation can be reproduced through the systematic skew quadrupole component.

This is however in contradiction with the counting of the number of invariants imposed by Hamiltonian Mechanics. As can be shown, two invariants exist for hamiltonian systems with two degrees of freedom: the volume of the four-dimensional phase-space and the sum of the projections onto each coordinate plane of any two-dimensional surface in the four-dimensional phase-space[14]. From this counting, one expects eight degrees of freedom for the fully coupled four-dimensional phase-space. We have not resolved this discrepancy.

In the special case of equal initial emittances in both planes ($r = 1$), our cal-

† With in both cases the same sign skew quadrupole component in the focusing and in the defocusing quadrupoles.

culations show that the fully coupled four-dimensional phase-space has six degrees of freedom. This is in agreement with an independent proof[15], and has also been verified in extensive computer simulations of optical corrections in the Final Focus System[16].

II.9 Case of the SLC Arcs

Not all perturbations are equally important in the case of the SLC Arcs.

Effects from the systematic coordinate rotation can in the SLC be ignored for all practical purposes, because the magnitude of the rotation angle can never be very large: for skew focusing errors of one percent, the rotation angle is only 1.15 degree.

In addition, effects on the phase-space from both the systematic skew quadrupole perturbation and the overall coordinate rotation are vanishing if the beam has, as is nominally specified, equal emittances in both planes.

In the case of the systematic skew quadrupole perturbation, there can however be significant effects on the betatron oscillations and on the transfer matrix. For beams with unequal emittances, the beats which are produced in each of the two emittances out of phase and are bounded by the larger emittance (see equation (25)). In the case of the SLC, where beams with emittance ratios of about one to three are presently measured at the end of the Linac, this is not a large effect*.

Effects from systematic focusing errors, over the whole length of the Arc, in the focusing and in the defocusing quadrupoles, would be small in entirely flat Arcs, except for mixing effects with the other perturbations. In the original design, the Arcs were rolled around their axis to enable following the terrain of the SLAC site, and this generated a strong sensitivity to systematic focusing errors. With the adiabatic roll transition which was introduced to remedy this problem, such systematic errors will produce coupling effects similar to the ones produced by a systematic skew focusing perturbation[17]. In the case of close to equal emittances, the effects on the phase-space from this are small, as was described above, and the modified Arcs have sensitivities which are similar to those of a flat Arc.

---

* This argument ignores mixing effects between several perturbations. It has in particular been shown that the upper bound described above can be significantly larger if the systematic skew deviation is mixed with a systematic phase difference between the motions in both planes and a one-dimensional mismatch from regular quadrupole errors[13].

II.10 Bandwidth Limits

The effect from the focusing modulation at the second harmonic of the betatron frequency, corresponding to $\nu = 2$, is weakened if a systematic focusing deviation, corresponding to $\nu = 0$, is simultaneously present, from either the errors in the array, or applied externally. This results from the gradual phase-shift which accumulates in this case between the resonantly growing optical mismatch and the induced focusing modulation (see Fig. 2). The mixing between the two perturbations will cause the resonant growth of the oscillations to reach a maximum and to then decay, in a long-range beating effect. The nominal phase-space will be fully restored when the phase-shift between the resonantly growing optical mismatch and the induced focusing modulation reaches π.

We will not derive the explicit form of the perturbed solution. We can however evaluate, at any given point along the array, the reduction in the growth of the oscillation amplitudes, by considering the modulation in frequency domain. The harmonic strength - or spectrum - of the focusing perturbation introduced along the array is given by the modulus of the Fourier transform of the perturbation. Here, we consider periodic perturbations - or modulations - which are applied along an array with finite length, corresponding to a total phase shift of $\phi_{max} = n\mu$, where μ is the phase-shift per cell, and n is the number of cells in the array. The harmonic strength is therefore given by:

$$\left|\mathcal{F}[d_{n\mu}(\phi) g e^{i\nu_{pert}\phi}]\right| = \left|g\delta(\nu - \nu_{pert}) \otimes \frac{\sin[n\mu\pi\nu]}{n\mu\pi\nu}\right|$$
$$= \left|g\frac{\sin[n\mu\pi(\nu - \nu_{pert})]}{n\mu\pi(\nu - \nu_{pert})}\right|, \qquad (32)$$

where $\delta(\nu)$ is the Dirac distribution, $\otimes$ symbolizes the convolution product, and $d_{n\mu}(\phi)$ is a function of ϕ which is equal to unity between 0 and $n\mu$, and zero everywhere else*.

This calculation is illustrated in Fig. 3. The range $\Delta\nu$ over which the harmonic strength is still reasonably large is given by about half the separation between the zeros of the function in (32), or $\Delta\nu = \pm 1/2n\mu$ cycles per radians. This corresponds to a maximum phase-shift of $\frac{\pi}{2}$, accumulated between the growing mismatch and

* This function is usually called the "door" function.

the focusing modulation, along the total length of the array, or to a maximum systematic phase-error per cell of:

$$\Delta\mu_{max} = \frac{\pi}{2n}. \tag{33}$$

Equation (33) gives the requirement on systematic errors in the array, as a function of its length, to maintain strong effects from the induced focusing modulation. The system of harmonic focusing corrections installed in the SLC Arcs extends over seven achromats, or $n = 70$ cells. The requirement on systematic phase-errors is in this case $\Delta\mu_{max} = \pm 1.3^0$ per cell.

III. HARMONIC PERTURBATIONS IN THE SLC ARCS

III.1 Definitions

A systematic perturbation in the focusing or in the defocusing magnets means that each focusing or defocusing magnet is perturbed the same way.

The cell phase-shift in the SLC Arc lattice is 108^0 or $\frac{3\pi}{5}$. Thus a perturbation at twice the betatron frequency is a perturbation whose strength is modulated by $\exp(i\frac{6\pi}{5}k)$ along the cells in the array, where k is the cell number.

A total of nine* independent harmonic perturbations can be generated in the SLC Arc lattice. We will represent the strength perturbations in the focusing and defocusing magnets respectively by F and D. We have:

1. Cosine-like in-plane (regular) horizontal second harmonic component:

$$F(k) = g_2^r \cos(\frac{6\pi}{5}k)$$

2. Sine-like in-plane (regular) horizontal second harmonic component:

$$F(k) = g_2^r \sin(\frac{6\pi}{5}k)$$

3. Cosine-like in-plane (regular) vertical second harmonic component:

$$D(k) = g_2^r \cos(\frac{6\pi}{5}k)$$

---

* Only nine adjustments can be generated, out of the ten which are needed to fully control the optical transfer. The missing one would be a regular focusing perturbation, as in 7. below, but with the same sign in the focusing and in the defocusing magnets. Such a perturbation can be generated electrically through the harmonic correction system described in this note, or through the already installed backleg windings, but has no optical effects because of the achromaticity of the lattice. The only way in which it can be generated in the SLC lattice is physically moving the focusing magnets closer or farther horizontally from the defocusing magnets.

4. Sine-like in-plane (regular) vertical second harmonic component:

$$D(k) = g_2^r \sin(\frac{6\pi}{5}k)$$

5. Cosine-like cross-plane (skew) second harmonic component:

$$F(k) = D(k) = g_2^s \cos(\frac{6\pi}{5}k)$$

6. Sine-like cross-plane (skew) second harmonic component:

$$F(k) = D(k) = g_2^s \sin(\frac{6\pi}{5}k)$$

7. Systematic regular focusing strength difference between focusing and defocusing magnets (*FD-Imbalance*):

$$F(k) = -D(k) = g_0^r$$

8. Systematic skew focusing perturbation in the focusing and defocusing magnets:

$$F(k) = D(k) = g_0^s$$

9. Overall coordinate rotation:

$$F(k) = -D(k) = g_0^s$$

III.2 Strength Perturbations in the Alternating Gradient Magnets

III.2.1 Backleg Wiring Modification

The combined function magnets in the Arc lattice are equipped with backleg windings on each coil. These backleg windings have 29 turns and are connected in series along one achromat. Their purpose is to provide a step-wise adaptation of the lattice to the energy of the beam, which loses about 1 Gev through the emission of synchrotron radiation in the guide-field. The strengths of each magnet in the 7 last achromats are perturbed individually by separately connecting and powering 4 out of 29 backleg winding turns on the upper and lower coils. The remaining 24 turns* are connected as for the original use of the backleg windings. A schematic of the modified wiring arrangement is shown in Fig. 4.

III.2.2 Strength Calculation

The separate four-turn-windings are inter-connected to produce periodic and systematic perturbations along the 7 last achromats in a way which we will describe below. Each circuit is presently powered with bi-polar HCOR12 supplies limited to ± 5 amperes by the voltage requirement. With four turns in each circuit and with the main Arc magnets powered with about 4000 amperes, the maximum strength perturbation of each magnet is of the order of ± 0.005.

More precisely, the magnitudes of the nominal and incremental dipole and quadrupole components† which are generated on the central trajectory have been calculated with POISSON, for Arc-type magnet, nominally powered with 3766 amperes in the main coil, and trimmed with 20 ampere-turns in the backleg windings[5].

When the top and bottom windings are perturbed with the same polarity, mid-plane symmetry is preserved and the strengths of the horizontally deflecting dipole field (vertical magnetic field), and of the regular quadrupole component in the combined function magnets are perturbed.

When the top and bottom windings are perturbed with opposite polarity, a vertically deflecting dipole field (horizontal magnetic field), and a skew quadrupole component are generated. The magnitudes of the components are listed below:

1. Nominally powered magnet: horizontal dipole = 5701.60 Gauss, regular quadrupole = 715.64 Gauss/mm.

2. Trimmed magnet with same polarity for top and bottom coils: incremen-

* The bottom windings on each coil have in some magnets been observed to droop and to cause partial shorts. As a preventive measure, the last turn was cut off and disconnected on each of the modified coils.

† We neglect the perturbation to the sextupole component, which is very small (less that 0.005 of the nominal value) and for which the tolerance for sizeable effects on the beam is loose (a few percent).

tal horizontal dipole = 27.87 Gauss, incremental regular quadrupole = 3.49 Gauss/mm. The magnitudes of the perturbations are close to equal in the focusing and defocusing magnets, and correspond to a 0.00488 of the nominal values.

3. Trimmed focusing magnet with opposite polarity for top and bottom coils: incremental vertical dipole = 14.05 Gauss, incremental skew quadrupole = 1.59 Gauss/mm. This corresponds to 0.0022 of the nominal values.

4. Trimmed defocusing magnet with opposite polarity for top and bottom coils: incremental vertical dipole = 16.58 Gauss, incremental skew quadrupole = 2.15 Gauss/mm. This corresponds to 0.0030 of the nominal values.

It can be noted that the skew components have about half the strength of the regular components. In addition, the magnitudes of the effects from trimming the focusing and defocusing magnets with opposite polarity for top and bottom coils are slightly assymetric. This may arise from an assymetry in the pole shape which exists between the two magnets.

III.2.3 Polarities of Components

We use the TRANSPORT polarity convention[11]. We have determined that:

1. A positive trim current in both top and bottom coils, to generate regular quadrupole components, will strengthen both focusing and defocusing magnets. This means that both the total bending angle and quadrupole component become stronger.

2. A positive trim current in the top coil and a negative trim current in the bottom coil, to generate skew quadrupole components, will generate a negative vertical kick in the defocusing magnets, a positive kick in the focusing magnets, and a negative skew quadrupole in both focusing and defocusing magnets.

III.3 Magnet Interconnections - Wiring and Layout

III.3.1 Intermagnet Wiring

Each trim winding, top or bottom, is connected in series with equivalent windings, top or bottom, exactly five cells (corresponding to 3π betatron phase-advance) (or ten magnets) apart, along the 7 last achromats (70 cells or 140 magnets) in the

Arcs. Since focusing and defocusing magnets are wired separately, there are thus 20 independent circuits. The wiring arrangement is illustrated in Fig. 5.

III.3.2 Nomenclature

The database formal names for the 20 supplies are listed below.

SMPS,CA13,1703=Top coil of defocusing magnet.

SMPS,CA13,1704=Bottom coil of defocusing magnet.

SMPS,CA13,1708=Top coil of focusing magnet.

SMPS,CA13,1709=Bottom coil of focusing magnet.

SMPS,CA13,1713=Top coil of defocusing magnet.

SMPS,CA13,1714=Bottom coil of defocusing magnet.

SMPS,CA13,1718=Top coil of focusing magnet.

SMPS,CA13,1719=Bottom coil of focusing magnet.

SMPS,CA13,1723=Top coil of defocusing magnet.

SMPS,CA13,1724=Bottom coil of defocusing magnet.

SMPS,CA13,1728=Top coil of focusing magnet.

SMPS,CA13,1729=Bottom coil of focusing magnet.

SMPS,CA13,1733=Top coil of defocusing magnet.

SMPS,CA13,1734=Bottom coil of defocusing magnet.

SMPS,CA13,1738=Top coil of focusing magnet.

SMPS,CA13,1739=Bottom coil of focusing magnet.

SMPS,CA13,1743=Top coil of defocusing magnet.

SMPS,CA13,1744=Bottom coil of defocusing magnet.

SMPS,CA13,1748=Top coil of focusing magnet.

SMPS,CA13,1749=Bottom coil of focusing magnet.

The last digit of the unit number (3,4,8,9) refers to top or bottom windings and to focusing and defocusing magnets. The next to last digit (0,1,2,3,4) refers

to the cell number of the first coil in the each string. The first two digits (17) refer to the achromat number of the first coil on each string.

III.3.3 Multiknob Definitions

The nine harmonic perturbations defined in III.1 are produced by linearly combining the 20 above supplies according to the coefficients given in the same paragraph, using the software multiknob facility[16]. The table below gives the mapping relating the 20 supplies to the 9 knobs:

	SINXX	COSXX	SINYY	COSYY	SINXY	COSXY	SYSKEW	SYSROT	FDIMB
1703	+0.00	+0.00	-0.59	-0.81	-0.59	-0.81	+1.00	+1.00	+1.00
1704	+0.00	+0.00	-0.59	-0.81	+0.59	+0.81	-1.00	-1.00	+1.00
1708	-0.59	-0.81	+0.00	+0.00	-0.79	-1.09	+1.35	-1.35	-1.00
1709	-0.59	-0.81	+0.00	+0.00	+0.79	+1.09	-1.35	+1.35	-1.00
1713	+0.00	+0.00	+0.95	+0.31	+0.95	+0.31	+1.00	+1.00	+1.00
1714	+0.00	+0.00	+0.95	+0.31	-0.95	-0.31	-1.00	-1.00	+1.00
1718	+0.95	+0.31	+0.00	+0.00	+1.28	+0.42	+1.35	-1.35	-1.00
1719	+0.95	+0.31	+0.00	+0.00	-1.28	-0.42	-1.35	+1.35	-1.00
1723	+0.00	+0.00	-0.95	+0.31	-0.95	+0.31	+1.00	+1.00	+1.00
1724	+0.00	+0.00	-0.95	+0.31	+0.95	-0.31	-1.00	-1.00	+1.00
1728	-0.95	+0.31	+0.00	+0.00	-1.28	+0.42	+1.35	-1.35	-1.00
1729	-0.95	+0.31	+0.00	+0.00	+1.28	-0.42	-1.35	+1.35	-1.00
1733	+0.00	+0.00	+0.59	-0.81	+0.59	-0.81	+1.00	+1.00	+1.00
1734	+0.00	+0.00	+0.59	-0.81	-0.59	+0.81	-1.00	-1.00	+1.00
1738	+0.59	-0.81	+0.00	+0.00	+0.79	-1.09	+1.35	-1.35	-1.00
1739	+0.59	-0.81	+0.00	+0.00	-0.79	+1.09	-1.35	+1.35	-1.00
1743	+0.00	+0.00	+0.00	+1.00	+0.00	+1.00	+1.00	+1.00	+1.00
1744	+0.00	+0.00	+0.00	+1.00	+0.00	-1.00	-1.00	-1.00	+1.00
1748	+0.00	+1.00	+0.00	+0.00	+0.00	+1.35	+1.35	-1.35	-1.00
1749	+0.00	+1.00	+0.00	+0.00	+0.00	-1.35	-1.35	+1.35	-1.00

Only seven of these nine knobs have been connected and used. The two missing ones are the second harmonic skew modulations: SINXY and COSXY. It can be noted that for the skew multiknobs, the focusing magnets have coefficients which are scaled by a factor of 1.35 with respect to those of the defocusing magnets, in order to account for the assymetry between the skew components which was noted in III.2.2

IV. SIMULATION OF EFFECTS

IV.1 Introduction to Simulation

We have used ARCSIM1[19] and TRANSPORT[11] to simulate the effects from focusing perturbations at zero and twice the betatron frequency.

ARCSIM1 is a fast simulation which treats small perturbations of the Arc magnets through a linear expansion around the design optical transfer matrix. The overall perturbed optical transfer is then reconstructed by multiplying each individually perturbed Arc matrix.

ARCSIM1 is ideally suited to study the physics of the harmonic focusing perturbations. However, in its current version, ARCSIM1 does not include steering effects from the combined function magnets. Such steering effects do not modify the physics but do modify the magnitude of the effects. In effect, through the sextupole component in the combined function magnets, horizontal deflections will cause regular quadrupole perturbations and vertical deflections will cause skew quadrupole perturbations. Because the strength perturbations are at zero or twice the betatron frequency, the trajectory excursions from these deflections, and the induced optical effects, will also be at zero or twice the betatron frequency. The optical effects will thus add to or subtract from the optical effect from the perturbations of the quadrupole components themselves. In addition, the perturbations will also cause net trajectory deviations* at the end. As will be seen, the trajectory deviations are large enough to require a correction. To correctly estimate the magnitude of the combined effects, we have used a perturbed TRANSPORT deck of the Arcs, in second order and including steering effects.

We first show the maximum effects of the first order optical distortions from the nine multiknobs defined above, in a perfect planar SLC Arc lattice. We do not consider second order optical distortions which arise from deviations in the achromaticity of the optical transfer caused by the first order distortions. Such effects have not been calculated in detail, but are estimated to be small.

Effects from rolls, which are present in the stretch of Arc lattice where the harmonic correction is introduced, will result in not fully orthogonal controls. The

* In theory, trajectory deviations would be resonant if the deflections were at the betatron frequency, and not at zero or twice the betatron frequency. In reality, because of the phase-slippage induced by the second harmonic (see II.6.1), the steering effects will grow slightly as the cancellations of deflections π apart no longer occur perfectly.

magnitude of the effects is however not strongly affected, since the component of the perturbed phase-space which is coupled into the other plane across each roll is not driven in that plane. In addition the component of the perturbed phase-space which is coupled into the other plane is not very large. To illustrate this point, we show the magnitude of one of the optical distortions in a lattice with the actual rolls installed in the present North Arc.

The plots shown are made with ARCSIM1, but the strengths of the knobs have been adjusted so that the maximum effect at the end of the seven achromat long stretch corresponds to the magnitude calculated with TRANSPORT, including the steering effects (this fudging exercise has however not been done for the phasing of the knobs).

We then show one simulated example of empirically correcting a lattice perturbed by errors with the harmonic correctors defined above. In the case of a systematic regular focusing error, we also illustrate the bandwidth limit discussed in II.10.

IV.2 Simulated Effects of Harmonic Correctors

IV.2.1 One-Dimensional Oscillations

Case $\nu \simeq 0$: *FD-Imbalance*

A nominal horizontal oscillation is shown in Fig. 6a. The same oscillation, but with the focusing and defocusing magnets perturbed through systematic regular focusing errors of ± 0.005 respectively is shown in Fig. 6b. As can be seen the amplitude of this oscillation is perturbed negligibly, but its frequency is shifted. It can be calculated that the corresponding shift, including optical effects from the displacement of the trajectory, is[9]:

$$(\Delta\mu_x, \Delta\mu_y) \simeq (\pm 87\,\text{deg}, \mp 115\,\text{deg}).$$

The trajectory displacement can also be calculated: it is 42μm[9]. Both agree well with simulated values.

A plot of the unperturbed and perturbed horizontal beam envelopes is shown in Fig. 7a,b. As can be seen, the beam envelopes are negligibly perturbed.

Case $\nu \simeq 2$: *Regular Second Harmonic*

Two one-dimensional horizontal oscillations with the same initial amplitude, but with two different initial phases separated by 90 deg, and with the focusing

magnets perturbed through regular focusing periodic modulation at twice the betatron frequency, with amplitude ± 0.005, are shown in Fig. 8a,b. The two initial phases have been chosen to obtain a maximally growing and a maximally decaying oscillation. As can be seen, the predicted maximum growth is about a factor four. The beats generated in the horizontal and vertical beam envelopes are shown in Fig. 9a,b. As can be seen, the orthogonality of the focusing and defocusing magnets which was noted in II.4.1 is almost perfect (i.e. there is almost no effect on the vertical beam envelope). This orthogonality is however not fully preserved if rolls are present in the lattice. To illustrate this point, we show in 9c,d the beats produced in the horizontal and vertical beam envelopes, from the same perturbation as in 9a,b applied to the North Arc with the present roll configuration. A reduction of the effect in the horizontal plane and some coupling into the vertical plane can be seen*.

Identical effects can be obtained for vertical oscillations with the defocusing magnets perturbed through regular focusing periodic modulation at the twice the betatron frequency.

The displacement of the trajectory is nearly 300μm from these knobs. This is large and requires a correction at the very end in order to be able to launch into the Final Focus.

IV.2.2 Two-Dimensional Oscillations

Case $\nu \simeq 0$: *Systematic Skew Component*

The coupling of an initially fully horizontal oscillation into the vertical plane, from the systematic skew knob set to its maximum of 5 amperes, is shown in Fig. 10a,b. As can be seen the maximum effect is just under 50%, which is rather weak. The same coupling would be obtained for an initially fully vertical oscillation into the horizontal plane, and for any input phase of the oscillation.

Plots of the corresponding beam envelopes are shown†, for a nominal initial phase-space in the horizontal plane and for zero initial phase-space in the vertical plane (Fig. 11a,b), and for a nominal equal initial phase-space in both planes (Fig. 12a,b). These two cases correspond to the beating effect described in II.7.2 through (26) and (27) respectively. In the case of nominal initial phase-space in

* A slightly smaller effect from these rolls would have perhaps been seen if the harmonic correction had been installed in a region where the major rolls are matched. Such a region could have been the region between the beginning of achromat 14 and the end of achromat 20.

† In order to make the effects more visible, we have calculated the perturbations of the envelopes for a systematic skew perturbation with three times the maximum knob strength.

both planes (Fig. 12a,b), the envelopes are not perturbed, as was found in (27).

The displacement of the trajectory from setting this knob at its maximum of 5 amperes is about 30μm. This is a small effect (partly because the knob is weak).

Effects from the systematic coordinate rotation are very small and are not illustrated here.

Case $\nu \simeq 2$: *Skew Second Harmonic*

The coupling of an initially fully horizontal oscillation into the vertical plane resulting from the skew second harmonic knob set to its maximum of 5 amperes is shown in Fig. 13a,b*. As can be seen the maximum effect is quite small. The same coupling would be obtained for an initially fully vertical oscillation into the horizontal plane, and for any input phase of the oscillation.

Plots of the corresponding beam envelopes are shown†, for a nominal initial phase-space in the horizontal plane and zero initial phase-space in the vertical plane (Fig. 14a,b), and for a nominal initial phase-space in both planes (Fig. 15a,b). These two cases correspond to the exponentially growing cross-plane coupling effects which were described in II.7.2 through (30) and (31) respectively.

The displacement of the trajectory from setting this knob has not been calculated in detail but appears to be large enough to require a correction at the very end, to launch properly into the Final Focus System.

IV.3 Systems with Errors

IV.3.1 Bandwidth Limit from Systematic Error

In Fig. 9.a, we showed the beat in the one-dimensional horizontal beam envelope caused by a regular second harmonic focusing perturbation. In Fig. 16, we show the same envelope, but now perturbed also by a systematic focusing perturbation corresponding to 3^0 per cell, or about twice the maximum systematic perturbation which can be caused by the FD-Imbalance. This corresponds to just over twice the maximum cell phase-shift which can be allowed for the harmonic knobs to work properly, as stated in II.10 by (33). As can be seen, the growth

* The two skew second harmonic knobs have not been tried experimentally.

† In order to make the effects more visible, we have calculated the perturbations of the envelopes for a skew second harmonic perturbation with five times the maximum knob strength.

in the beating envelope is in this case reversed half way through, and is nearly cancelled at the end.

IV.3.2 Empirical Correction of Randomly Perturbed Lattice

Fig. 17 shows the horizontal beam envelope imaged through the seven achromat long stretch, perturbed by random regular focusing errors only, with strengths normally distributed with a standard deviation of 0.01. The particular "seed" shown in Fig. 17 was chosen as one which generates significant growth of about a factor two. With this magnitude error, such a large growth represents a rather improbable case*. Fig. 18 shows a correction of the case presented in Fig. 17, by combining the sine-like and cosine-like regular focusing second harmonic correctors. Correction is found empirically rather easily for such one-dimensional cases. In lattices fully perturbed with regular and skew focusing errors, the empirical method is in some cases difficult.

* As per IV.2.2, a factor two growth can be generated with a regular focusing modulation at twice the betatron frequency of amplitude 0.0025 (half the knob strength). For randomly distributed regular focusing errors with a standard deviation of 0.01, the one standard deviation expectation value for the strength of the component at twice the betatron frequency is $\frac{0.01}{\sqrt{n}} = 0.0012$, where $n = 70$ is the number of cells in the seven achromats. Thus a 0.0025 strength would correspond to about two standard deviations of the strength distribution, or about 5% of the seeds.

V. LIMITATIONS AND PROSPECTS

V.1 Strength Limitations

The strength of the controls provided in the installation described above is severely limited in the case of the cross-plane coupling correctors (the "skew knobs"). Stronger "systematic skew knobs" in particular would be important for future operation with assymetric emittances, to fully cancel the coupling between the two emittances. They do however not appear to be essential for the present operation with close to equal emittances, a case for which they have no or little effect on the beam envelope (see II.7.3).

In addition, in the presence of systematic regular focusing errors of more than one degree per cell, the strength of the correctors for one-dimensional mismatches are significantly weakened. More generally, the strengths of all the correctors are weakened by phase errors distributed in the stretch where the harmonic correction is installed.

V.2 Guide-line for Upgrade

The obvious upgrade would consist in raising the maximum current through the rewired backleg windings, from the present value of about 5 amperes, to twice or three times that. There may be an impediment to doing this from the limited elasticity in the copper wires composing the windings: after the controls have been turned on and off a large number of times, the repeated thermal contractions and dilatations may cause the windings to sag. An enhanced support mechanism would perhaps be required. The possibility of this sagging is presently being examined.

Another possible upgrade would consist in repeating the installation in one or two new stretches upstream of the one described above. Because of the observed tendency of the bottom turn of the backleg windings to droop (see the footnote at the bottom of page 22), it may be desirable, as a preventive measure, to implement the wiring modification in the remaining 16 achromats. In this case, two new installations similar to the one in achromats 17-23 could be installed in achromats 9-16 and in achromats 1-7. The existing supplies could in this case be kept, as knobs in adjoining stretches could be combined to enhance the effects. The drawback of this is evidently a much increased complexity, as one would then have to deal with

a theoretical* total of 27 knobs, with their relative phasing "and so on".

In summary, if the possible sag in the wires from heating can be solved with a better clamping mechanism, or otherwise shown not to be a problem, and if it is not essential to implement the wiring modification as a preventive measure for the sagging of the last wire, our recommendation would be to upgrade the power supplies.

V.3 Predictive and Precision Control

The harmonic corrections are presently performed successfully as approximate and empirical adjustments to control the beam shape at particularly sensitive places at the entrance to the Final Focus, where significant backgrounds can be generated by optical mismatches, or to adjust the overall lattice of the Arcs to be close to nominal[4].

More work would be required to design fully predictable model-driven corrections for precision control of phase-space parameters at the end of the Arcs. This may be doable by using empirically determined transfer matrices for the Arcs, together with a perturbation technique similar to the one described in IV.1[20]. Some attempts which were made in this direction have shown that this is not straightforward, and requires a detailed understanding of the propagation of measurement errors involved in the empirical matrix determination. More work in this direction may enable precision controlling the phase-space for future optical optimizations of the SLC Arcs.

* In practice, the coordinate rotations do not matter, so "only" 24 knobs would be used.

ACKNOWLEDGEMENTS

Several people have contributed to this work in a major way, and should be acknowledged. Rae Stiening was the first to propose harmonic corrections as a method for adjusting long open FODO arrays. Ted Fieguth pioneered the method in the case of the SLC Arcs, through a system of harmonic steering bumps.

In addition, we have benefited from discussions with Karl Brown, Fatin Bulos, Dave Burke, Dick Early, Jacques Haïssinski, Thomas Lohse, David Ritson, Matt Sands and Nobu Toge.

Finally, we would like to thank the Mechanical Engineering and Power Supply Groups, and the cable installation crews for their support in the installation of "Wirefix".

REFERENCES

(1) P. Bambade, "Beam Dynamics in the SLC Final Focus", SLAC-PUB 4227 (June 1987), C. Hawkes and P. Bambade, "First Order Optical Matching in the Final Focus Section of the SLAC Linear Collider", Nucl. Instr. and Meth. A274 (1989) 27 and P. Bambade *et al.*, "Operational Experience with Optical Matching in the SLC Final Focus System", SLAC-PUB-4776 January (1989).

(2) R. Stiening, "Focusing Errors in the SLC Linac Quadrupole Lattice", SLAC-CN-161 (February 1982).

(3) T. Fieguth, "Harmonic Orbit Distortions", Minutes of GIAT Group Meeting (October 1985).

(4) P. Bambade *et al.*, "Initial Operational Experience with Harmonic Corrections in the SLC Arcs", To be published at the Particle Accelerator Conference, in Chicago (March 1989).

(5) D. Early, "Steering Effects in the Main E Bend Magnet", SLAC-CN-216 (January 1983).

(6) P. Bambade, "Betatron Phase-space Diagnostic in a FODO Array", SLAC-CN-367 (October 1988).

(7) E. Courant and H. Snyder, "Theory of the Alternating Gradient Synchrotron", Ann. of Phys. 3,1-48 (1958).

(8) E. Brigham, "The Fast Fourier Transform", New Jersey, Prentice-Hall, Inc.

(9) J. Haïssinski, Private Communications (April 1987 through January 1989).

(10) A. Nayfeh, "Introduction to Perturbation Techniques", New York, Wiley (1981).

(11) K. Brown *et al.*, "TRANSPORT", SLAC-91, Rev. 2 (May 1977).

(12) E. Wilson, "Circular Accelerators-Transverse", AIP Conf. Proc. 153, p. 3, (1987).

(13) K. Brown and R. Servranckx, "Cross-Plane Coupling and its Effects on Projected Emittances", SLAC-PUB-4679 (July 1988).

(14) L. Teng, "Concerning N-Dimensional Coupled Motions", FermiLab Report FN-229 (May 1971).

(15) The first of the three references in (1).

(16) At this point, this is common knowledge.

(17) P. Bambade *et al.*, "Rollfix - An Adiabatic Roll Transition for the SLC Arcs", SLAC-PUB-4835 (January 1989). (18) Julian Kupiec, "User Guide to the Multiknob Facility".

(19) D. Ritson, ARCSIM, private program (March 1988). A modified version (ARCSIM1) exists with harmonic focusing corrections using regular quadrupoles. Both versions are installed on the shared SLC 197 disk.

(20) T. Barklow, "A Technique for Measuring the 4X4 Transfer Matrix for Beam-Line Sections with Cross-plane Coupling", To be published at the Particle Accelerator Conference, in Chicago (March 1989).

FIGURE CAPTIONS

(1) Mismatched one-dimensional phase-space. The beam-size beats between maxima and minima of M and 1/M respectively.

(2) If a systematic regular focusing error is present, the focusing modulation being applied and the beat of the beam size become gradually out of phase. This weakens the effect of the harmonic corrector.

(3) Harmonic strength associated to a focusing modulation over a finite length.

(4) Wiring modification of backleg trim windings. Four of the twenty-nine turns are connected to a separate circuit, via the upper right terminal. The twenty-five remaining turns are connected as for the original use of the backleg windings, via the top terminal, except for the bottom, which is removed from the circuit.

(5) There are twenty independent circuits connecting the 280 top and bottom coils of the last seven achromats in the Arcs. In each circuit, top and bottom coils of magnets separated by five cells are connected in series.

(6) Horizontal betatron oscillation in seven achromats of the SLC Arcs, with no errors (a), and with a 1% FD-Imbalance (b).

(7) Horizontal beam size in seven achromats of the SLC Arcs, with no errors (a), and with a 1% FD-Imbalance (b).

(8) Horizontal betatron oscillation in seven achromats of the SLC Arcs, with a cosine-like regular quadrupole modulation at twice the betatron frequency in the focusing magnets, corresponding to COSXX=5 Amperes, and for two initial phases amounting to maximum growth (a) and maximum decay (b).

(9) Horizontal and vertical beam sizes in seven achromats of the SLC Arcs, with a cosine-like regular quadrupole modulation at twice the betatron frequency in the focusing magnets, corresponding to COSXX=5 Amperes. Cases (a) and (b) correspond to respectively the horizontal and vertical beam sizes in entirely flat Arcs. As can be seen, the modulation affects mostly the horizontal motion. Cases (c) and (d) correspond to respectively the horizontal and vertical beam sizes in the last seven achromats of the North Arc, with the present roll distribution. As can be seen, some coupling is generated in the vertical plane, and the beats in the horizontal plane are weakened by about 25%.

(10) Horizontal (a) and vertical (b) betatron oscillation in seven achromats of the SLC Arcs, with a systematic skew focusing perturbation, corresponding to

SYSKEW=5 Amperes.

(11) Horizontal (a) and vertical (b) beam size in seven achromats of the SLC Arcs, with a systematic skew focusing perturbation, corresponding to SYSKEW=15 Amperes. In these plots, the initial emittance is zero in the vertical plane. An exchange of oscillation energy from the horizontal plane to the vertical plane can be seen.

(12) Horizontal (a) and vertical (b) beam size in seven achromats of the SLC Arcs, with a systematic skew focusing perturbation, corresponding to SYSKEW=15 Amperes. In these plots, the initial emittances are equal in the horizontal and vertical planes. In this case, the skew focusing perturbation has no effect on the beam envelopes.

(13) Horizontal (a) and vertical (b) betatron oscillation in seven achromats of the SLC Arcs, with a skew focusing modulation at twice the betatron frequency, corresponding to COSXY=5 Amperes.

(14) Horizontal (a) and vertical (b) beam size in seven achromats of the SLC Arcs, with a skew focusing modulation at twice the betatron frequency, corresponding to SYSKEW=25 Amperes. In these plots, the initial emittance is zero in the vertical plane. Growth of the phase-space in both the horizontal and vertical planes can be seen.

(15) Horizontal (a) and vertical (b) beam size in seven achromats of the SLC Arcs, with a skew focusing modulation at twice the betatron frequency, corresponding to SYSKEW=25 Amperes. In these plots, the initial emittances are equal in the horizontal and vertical planes. Growth of the phase-space in both the horizontal and vertical planes can be seen.

(16) Horizontal beam size in seven achromats of the SLC Arcs, with a cosine-like regular quadrupole modulation at twice the betatron frequency in the focusing magnets, corresponding to COSXX=5 Amperes, and with a systematic focusing perturbation of 1.33% in the focusing magnets. As can be seen, a beat in the beam size is initiated as in Fig. 9a, but is reversed in the middle of the section and vanishes almost at the end.

(17) Horizontal beam size in seven achromats of the SLC Arcs with the focusing magnets perturbed by random quadrupole errors with a 1% standard deviation. The particular "seed" was chosen as one which generates large beats at the end.

(18) Horizontal beam size in seven achromats of the SLC Arcs with the focusing magnets perturbed by the same random quadrupole errors as in (17), and corrected

by superimposing a quadrupole modulation at twice the betatron frequency in the focusing magnets, corresponding to COSXX=3.9 Amperes and to SINXX=0.7 Amperes. As can be seen, the correction is almost perfect at the end.

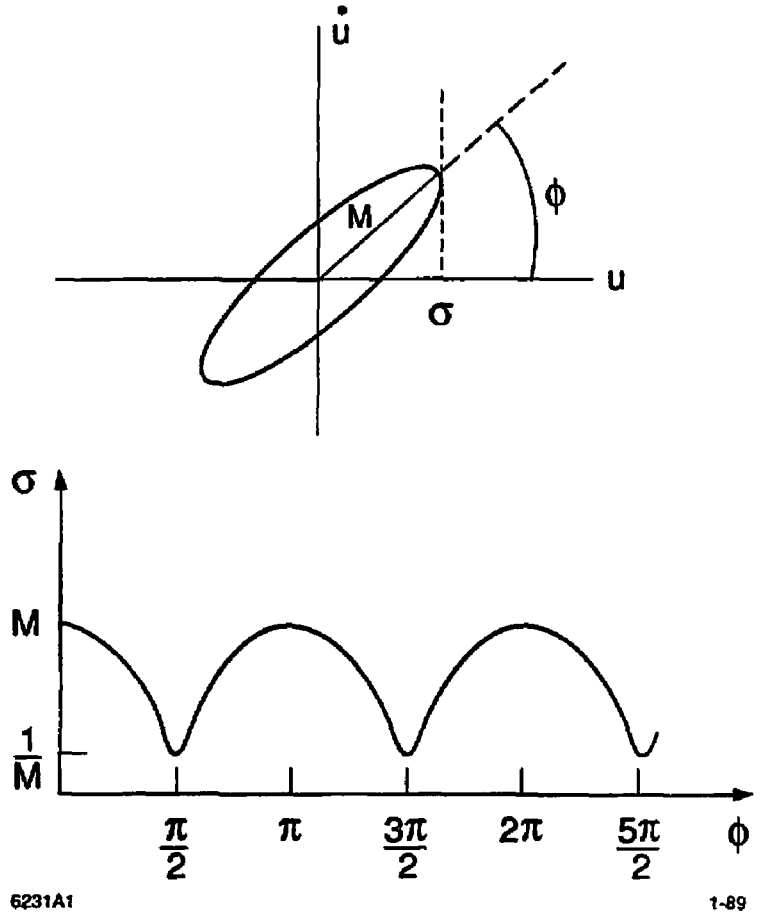

Fig. 1

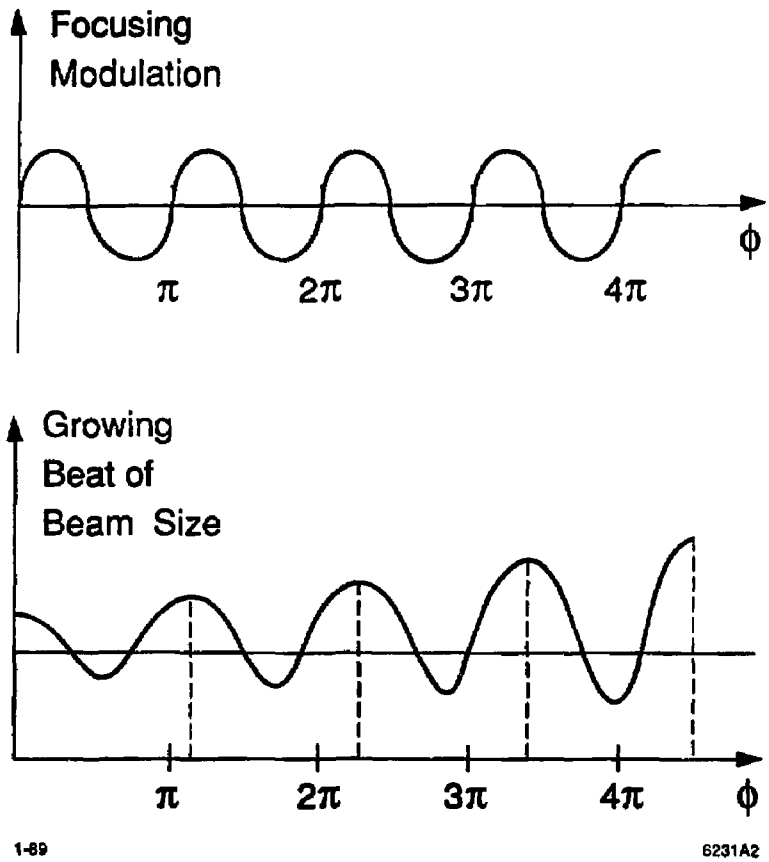
Focusing
Modulation
π
2π
3π
4π
ϕ
Growing
Beat of
Beam Size
π
2π
3π
4π
ϕ
1-89
6231A2

Fig. 2

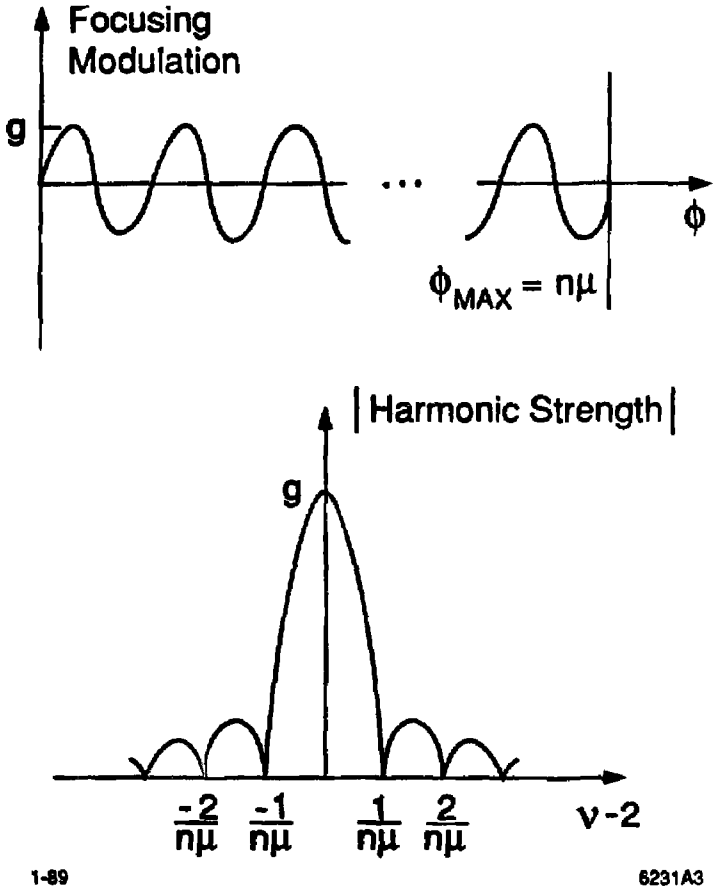
Focusing
Modulation
g
...
ϕ
ϕMAX = nμ
| Harmonic Strength |
g
-2/nμ
-1/nμ
1/nμ
2/nμ
ν-2
1-89
6231A3

Fig. 3

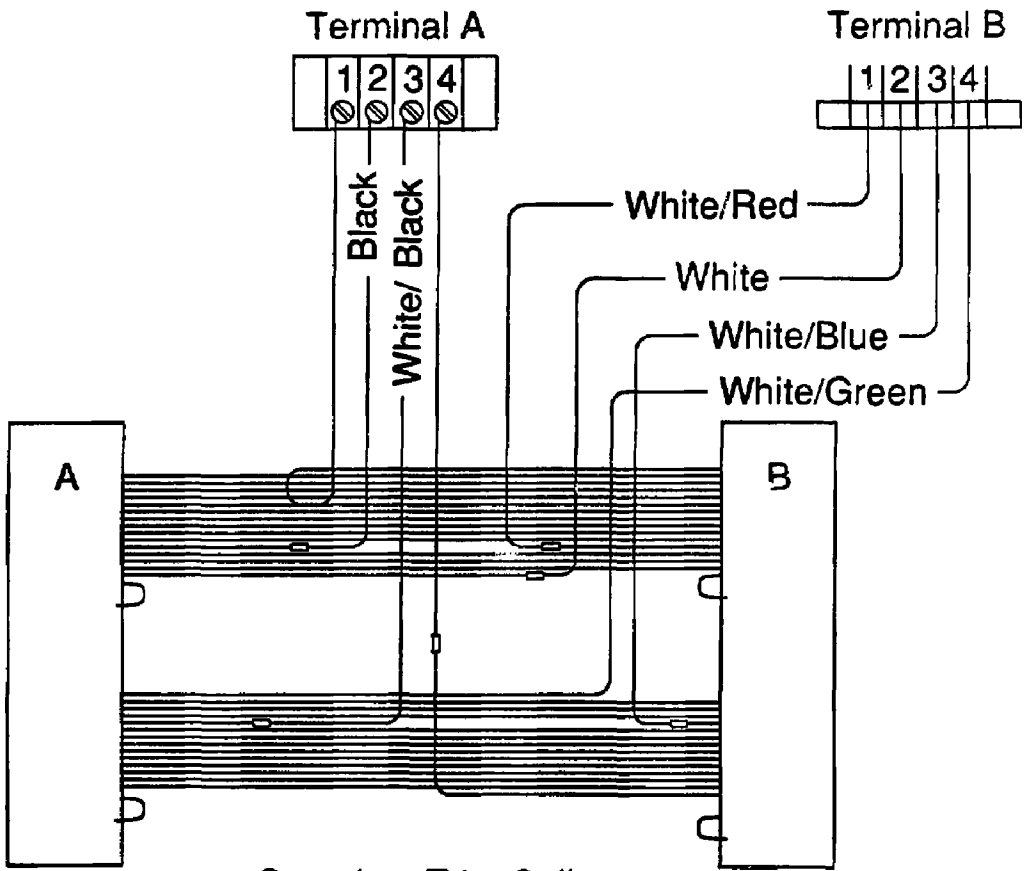
Terminal A
1
2
3
4
Terminal B
1
2
3
4
Black
White/ Black
White/Red
White
White/Blue
White/Green
A
B
Complete Trim Coil
After Wire Fix
1-89
6231A4

Fig. 4

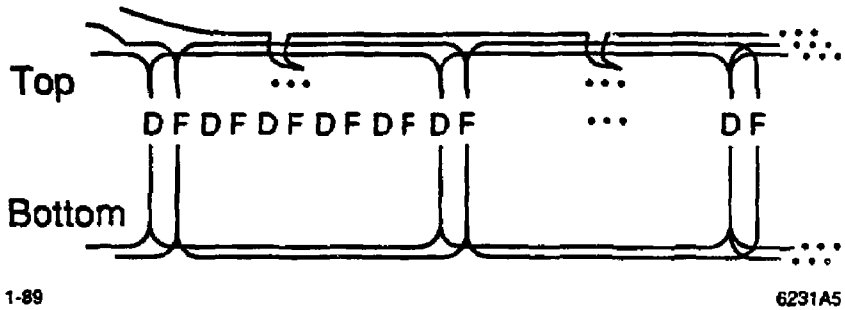

Fig. 5

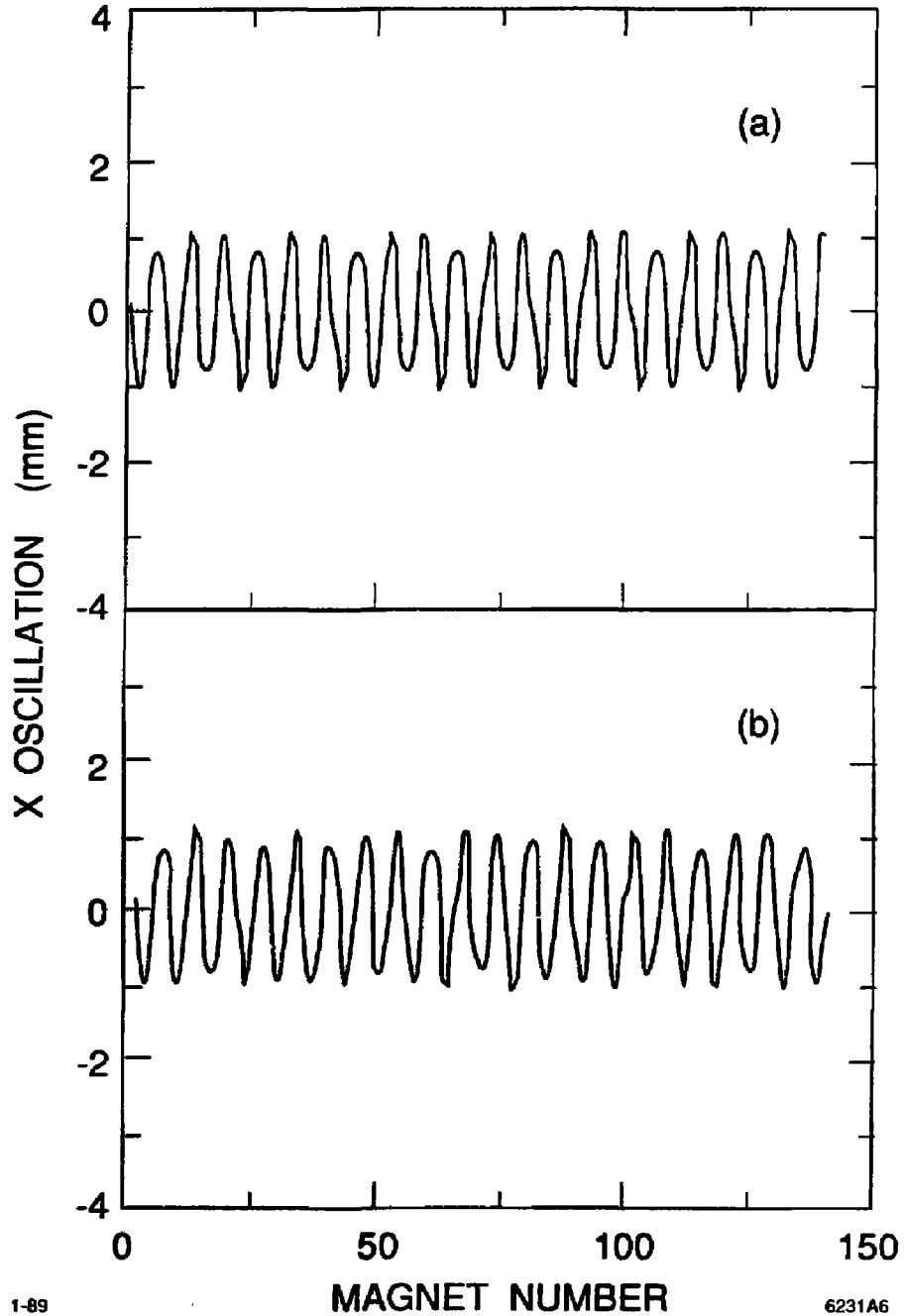

1-89 6231A6

Fig. 6

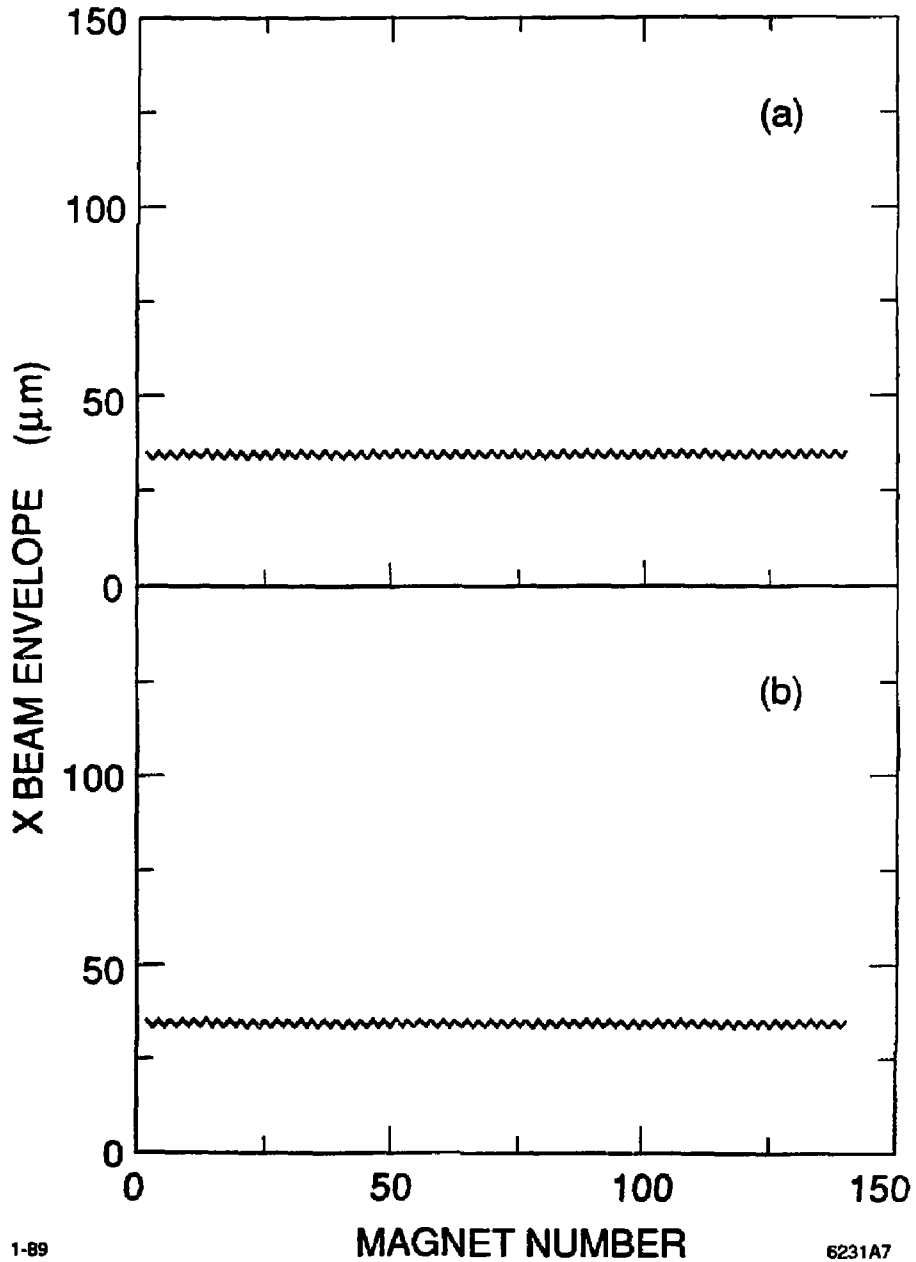
150
100
50
0
(a)
(b)
100
50
0
0
50
100
150
X BEAM ENVELOPE (μm)
MAGNET NUMBER
1-89
6231A7

Fig. 7

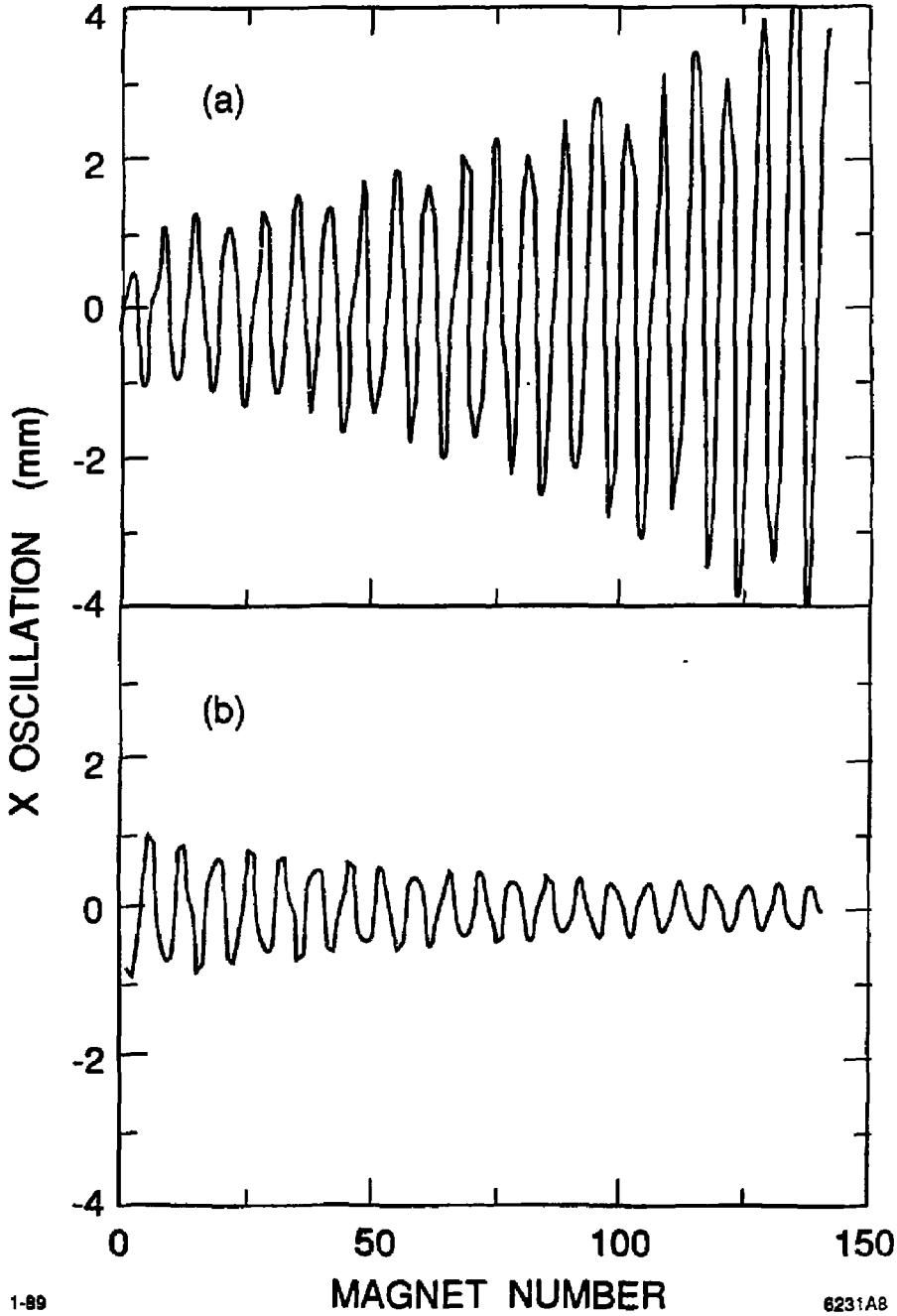
4
2
0
-2
-4
(a)
(b)
X OSCILLATION (mm)
0
50
100
150
MAGNET NUMBER
1-99
6231A8

Fig. 8

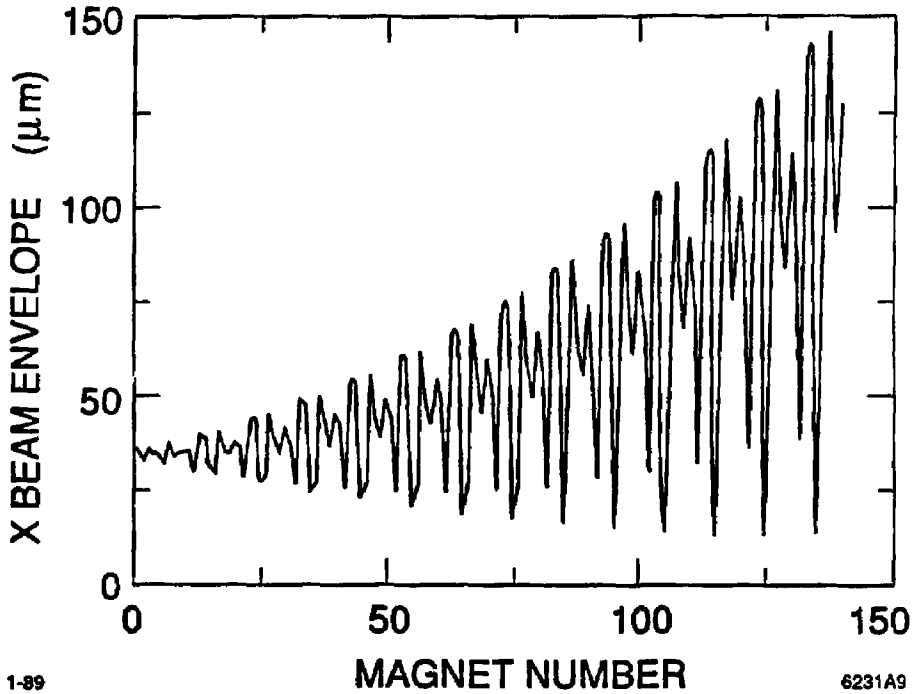
150
100
50
0
X BEAM ENVELOPE (μm)
0
50
100
150
MAGNET NUMBER
1-89
6231A9

Fig. 9

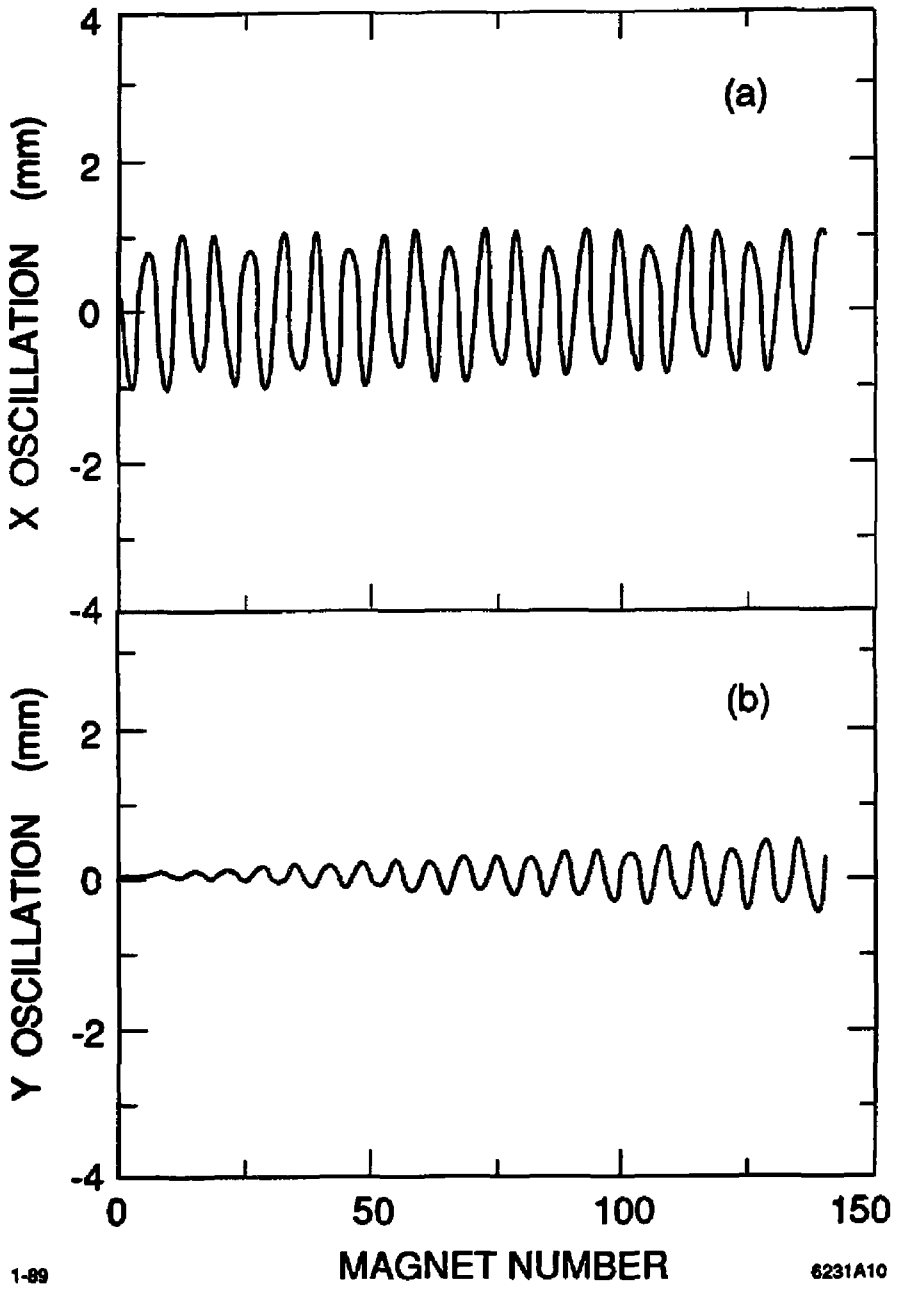
4
2
0
-2
-4
X OSCILLATION (mm)
(a)
4
2
0
-2
-4
Y OSCILLATION (mm)
(b)
0
50
100
150
MAGNET NUMBER
1-89
6231A10

Fig. 10

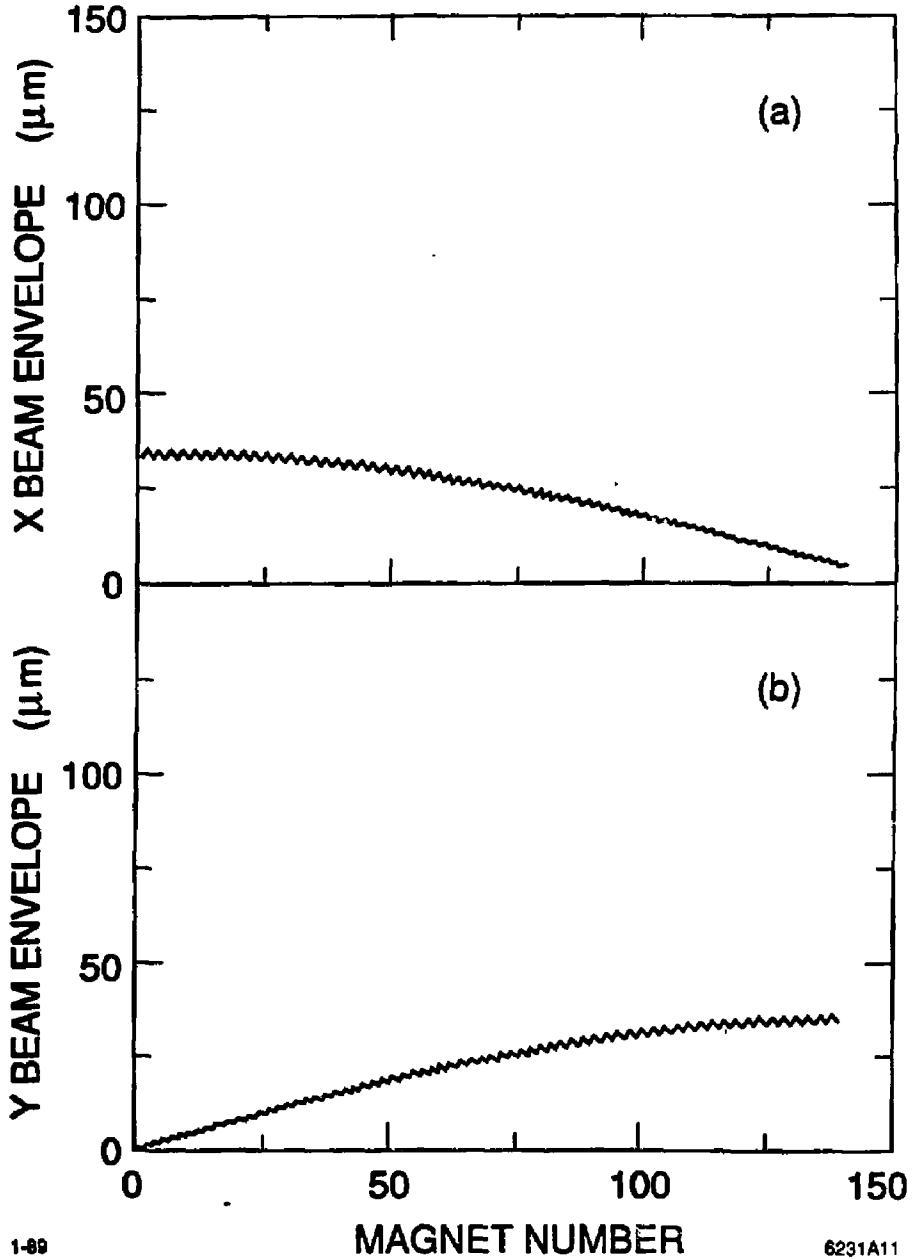
150
100
50
0
X BEAM ENVELOPE (μm)
(a)
150
100
50
0
Y BEAM ENVELOPE (μm)
(b)
0
50
100
150
MAGNET NUMBER
1-89
6231A11

Fig. 11

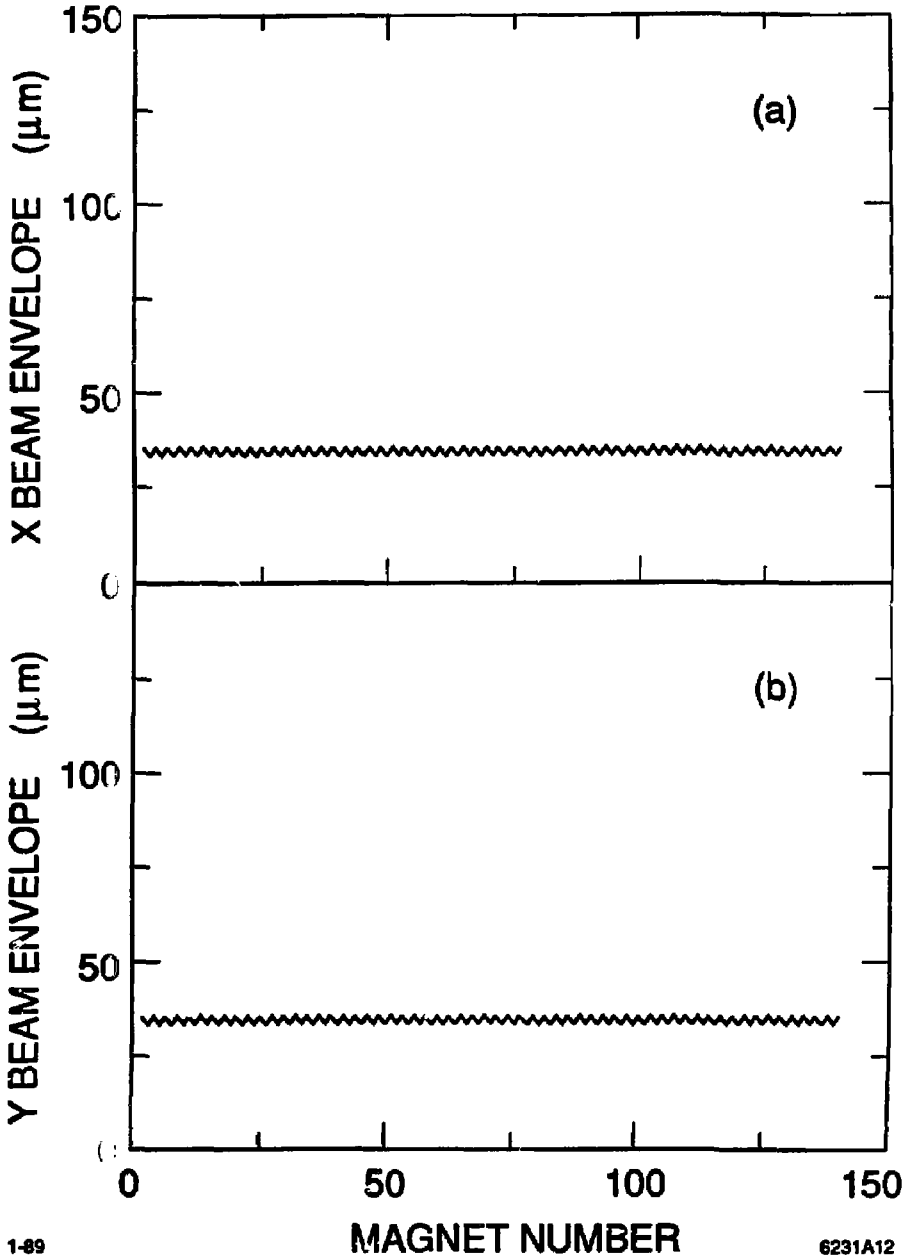
150
100
50
0
X BEAM ENVELOPE (μm)
(a)
100
50
0
Y BEAM ENVELOPE (μm)
(b)
0
50
100
150
MAGNET NUMBER
1-89
6231A12

Fig. 12

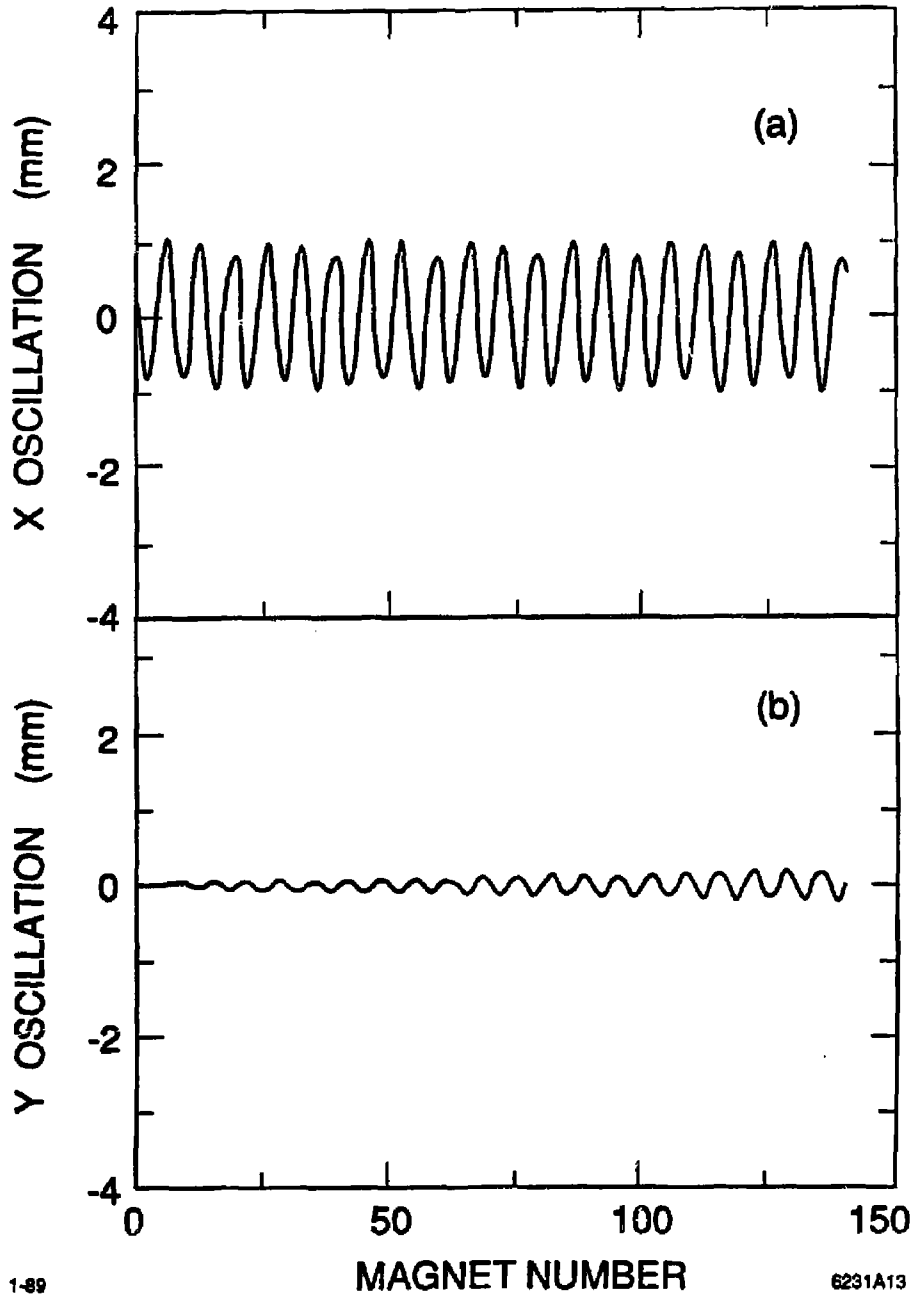
4
2
0
-2
-4
X OSCILLATION (mm)
(a)
2
0
-2
-4
Y OSCILLATION (mm)
(b)
0
50
100
150
MAGNET NUMBER
1-89
6231A13

Fig. 13

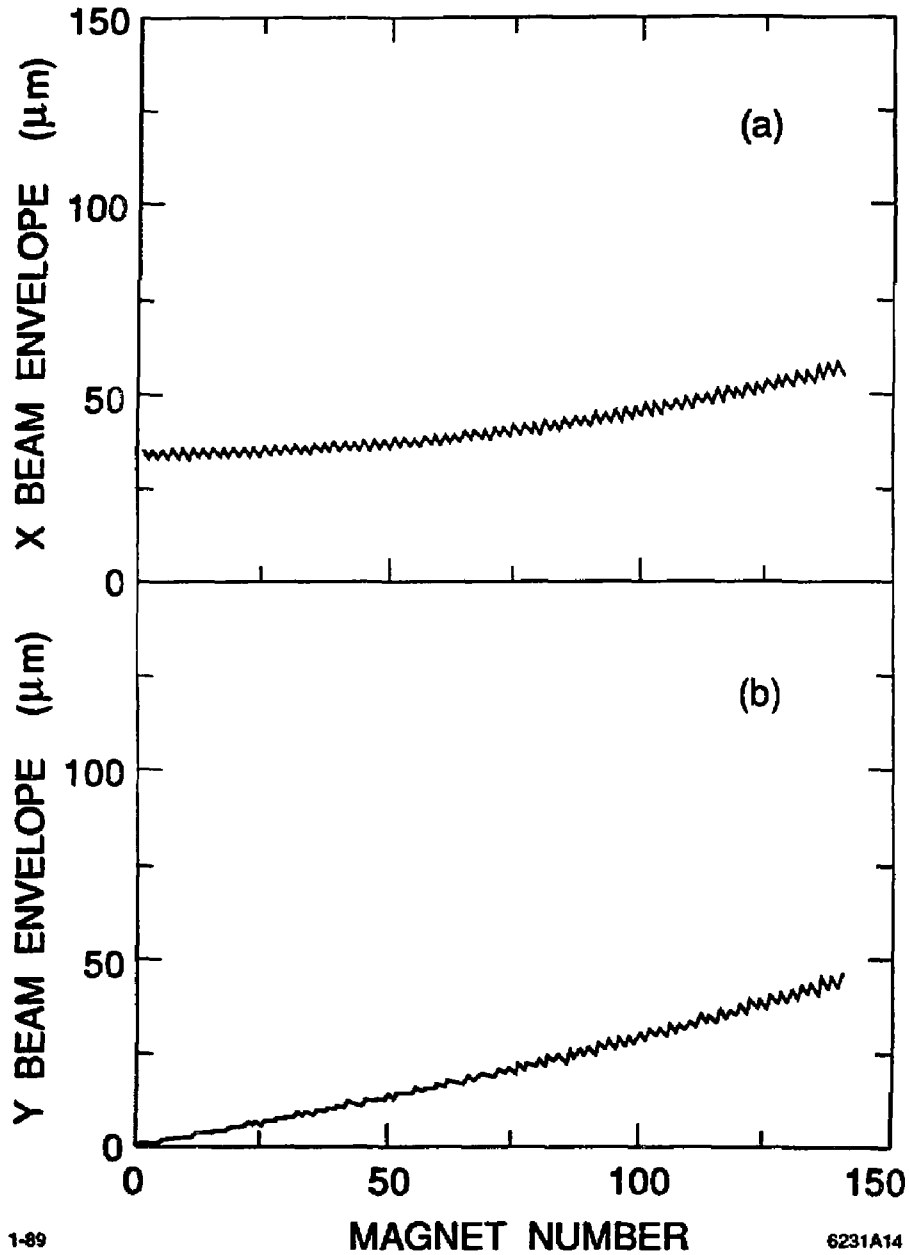
150
100
50
0
X BEAM ENVELOPE (μm)
(a)
150
100
50
0
Y BEAM ENVELOPE (μm)
(b)
0
50
100
150
MAGNET NUMBER
1-89
6231A14

Fig. 14

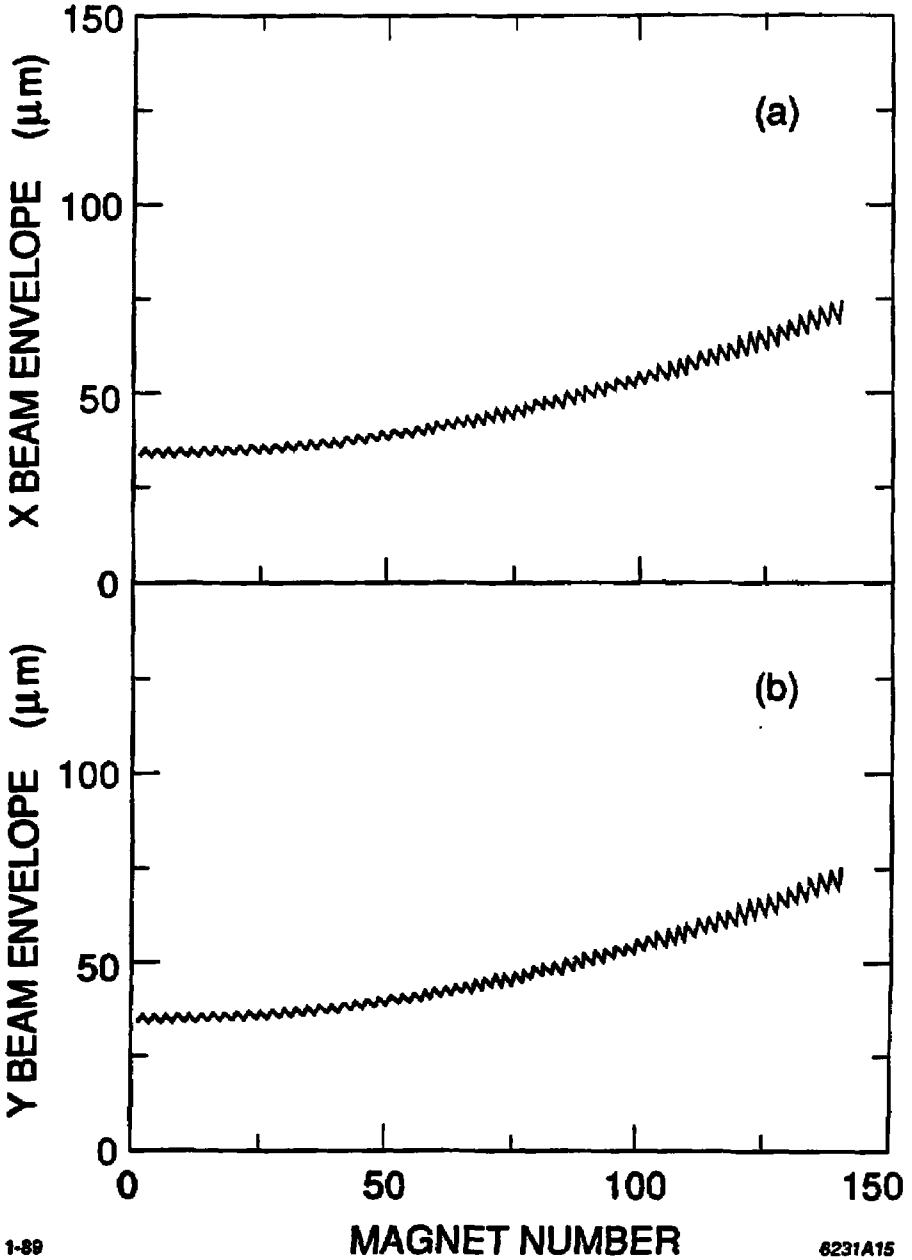
150
100
50
0
X BEAM ENVELOPE (μm)
(a)
(b)
Y BEAM ENVELOPE (μm)
0
50
100
150
MAGNET NUMBER
1-89
6231A15

Fig. 15

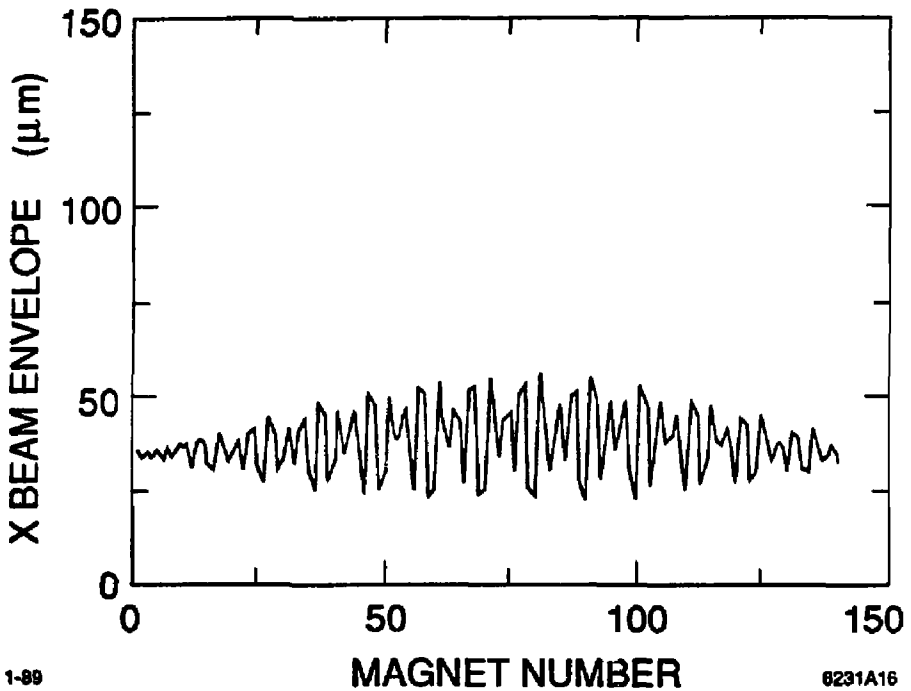
150
100
50
0
X BEAM ENVELOPE (μm)
0
50
100
150
MAGNET NUMBER
1-89
6231A16

Fig. 16

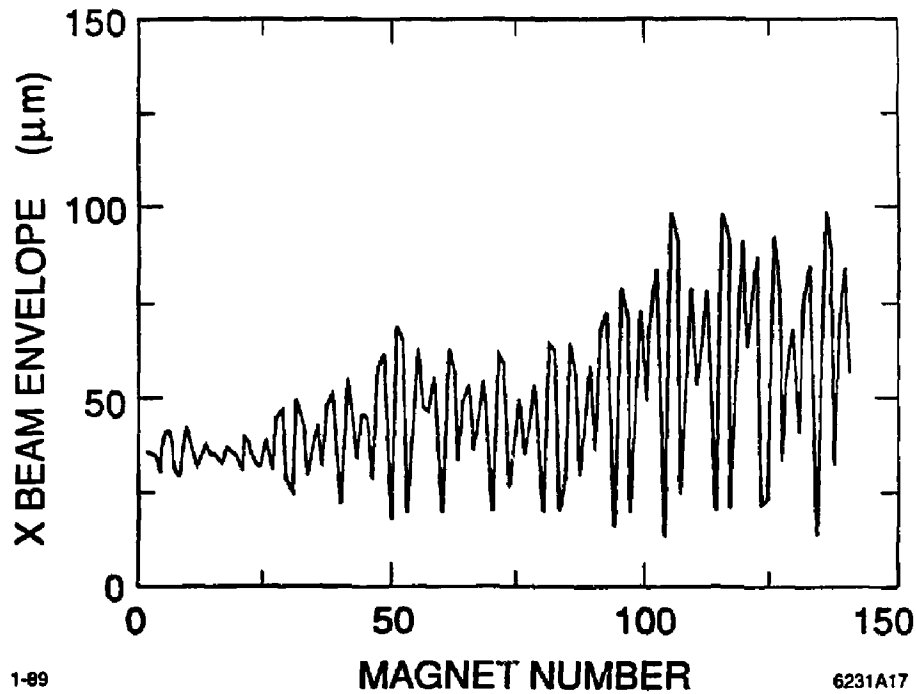
150
100
50
0
X BEAM ENVELOPE (μm)
0
50
100
150
MAGNET NUMBER
1-89
6231A17

Fig. 17

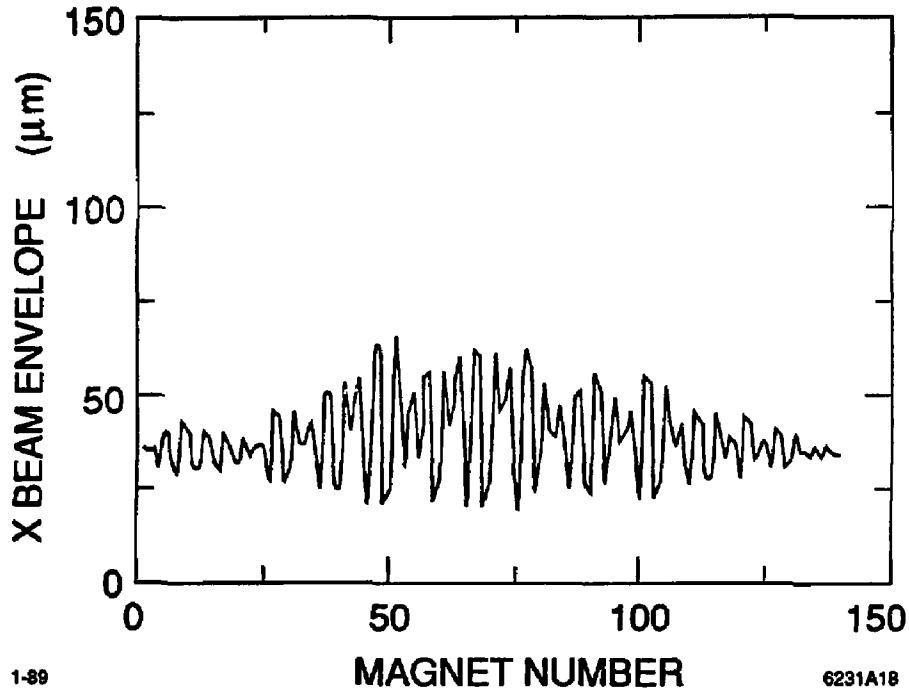
150
100
50
0
X BEAM ENVELOPE (μm)
0
50
100
150
MAGNET NUMBER
1-89
6231A18

Fig. 18